Hindawi Publishing Corporation
Advances in Civil Engineering
Volume 2011, Article ID 932871, 24 pages
doi:10.1155/2011/932871

Research Article

Multiobjective Design Optimization of Grillage Systems according to LRFD-AISC

Tugrul Talaslioglu

High Vocational School of Kadirli, Osmaniye Korkut Ata University, 80000 Osmaniye, Turkey

Correspondence should be addressed to Tugrul Talaslioglu, talaslioglu@cu.edu.tr

Received 9 November 2010; Revised 18 May 2011; Accepted 29 May 2011

Academic Editor: Manolis Papadrakakis

Both the entire weight and joint displacements of grid structures are minimized at the same time in this study. Four multiobjective optimization algorithms, NSGAII, SPEAII, PESAII, and AbYSS are employed to perform computational procedures related to optimization processes. The design constraints related to serviceability and ultimate strength of grid structure are implemented from Load and Resistance Factor Design-American Institute of Steel Constructions (LRFD-AISC Ver.13). Hence, while the computational performances of these four optimization algorithms are compared using different combinations of optimizer-related parameters, the various strengths of grid members are also evaluated. For this purpose, multiobjective optimization algorithms (MOAs) employed are applied to the design optimization of three application examples and achieved to generate various optimal designations using different combinations of optimizer-related parameters. According to assessment of these optimal designations considering various quality indicators, IGD, HV, and spread, AbYSSS shows a better performance comparatively to the other three proposed MOAs, NSGAII, SPEAII, and PESAII.

1. Introduction

The grillage systems utilized in different structures like bridge or ship decks, building floors and space buildings, and so forth, contain traverse and longitudinal beams, which are made of available steel profiles with different cross-sections. The optimal selection of steel cross-sections from a discrete set of practically available steel profiles provides a big contribution to constructing cost of a grid structure. Therefore, either weight of grid structure or deflection of its joints is minimized according to certain design limitations prescribed by any code of practice, such as LRFD. During the design optimization of grillage systems, designer is frequently faced with a problem related to making a decision about determination of the most appropriate one between these two conflicting and commensurable objective functions. Although a displacement-related constraint is imposed as a (max span/300) according to the provisions of LRFD-AISC specification, the safety margin on displacement constraint is large when taking into account the grid structures with higher sensitivity against displacement, such as ship decks and floors of industrial buildings which bears special machines required an horizontally balanced position for a regular work. This task has been easily overcome in a way of introducing the concept of multi-objective optimization to the design applications of grid systems.

Preliminary multi-objective optimization techniques, which their fundamentals were constituted on mathematical programming principles, were dated back to the 1950s. However, mathematical programming techniques adjust the decision variables of continuous type according to gradient information computed by use of objective functions. Furthermore, they fail when search space is concave and discontinuous. In order to deal with these tasks, alternative optimization procedures, which mimic various natural events, for example, evolutionary systems, immune systems, social behaviors of ants, insects, and animals, have been developed. The most preferable ones are the evolutionary-based algorithms. These biological evolutionary models utilize characteristic properties of nature, for example, heredity, selection, and so forth, to create populations with higher qualities. Particularly, genetic algorithms (GAs) are the most flexible multi-objective evolutionary tools due to allowing an implementation of various operators for its evolutionary

computation. Therefore, it has been hybridized with different local search techniques.

First study on the multiobjective evolutionary optimization, called Vector Evaluated Genetic Algorithm (VEGA) was performed by use of GA's principle [1]. VEGA employs a number of subpopulations to search the solution space considering a modified selection mechanism. Following the emergence of VEGA, two featured approaches, linear aggregating and lexicographic ordering of objective functions were developed [2, 3]. They transformed all objective functions into a single objective function by way of optimizing each objective function without decreasing their solution qualities.

As an alternative to early attempts mentioned above, a pareto-based evolutionary approach was developed to increase the population diversity [4]. Some of the preliminary pareto-based multi-objective optimization approaches are Nondominated Sorting Genetic Algorithm (NSGA) by Srinivas and Deb [5], a Niched Pareto Genetic Algorithm (NPGA) by Horn et al. [6], a Multi-objective Genetic Algorithm (MOGA) by Fonseca and Fleming [7], and a Multi-objective Evolutionary Algorithm (MOEA) by Tanaka and Tanino [8]. In order to improve their optimal results, these algorithms have been developed by either enhancing their current optimization strategies, such as Nondominated Sorting Genetic Algorithm II (NSGA II), Improved Strength Pareto Evolutionary Algorithm II (SPEA II), Improved Pareto Envelope-Based Selection Algorithm (Region-Based Selection) II (PESA II), or adapting a competitive Search Technique, such as Adapting Scatter Search AbYSS.

Although it is clear that there are a number of evolutionary methods known in the field of evolutionary multiobjective optimization, in this paper, an exhaustive literature review on this field is omitted. Instead, representative works related to four multi-objective optimization techniques employed are summarized. Furthermore, the recent multi-objective approaches utilized in the field of structural engineering design are also reviewed.

In this regard, paper is organized as firstly introducing the first steps in MOAs including applications in the field of structural engineering after a brief introduction to the multi-objective optimization problem and concepts. The computational procedures of proposed MOAs, NSGAII, SPEA II, PESA II, and AbYSS are presented in Section 3. The design requirements prescribed by LRFD-AISC Ver.13 and optimal design procedure are given in Section 4 prior to the introduction of search methodology located in Section 5. Following the discussion of results along presented in Section 6, final remarks are summarized in Section 7.

2. Background

2.1. Multiobjective Optimization: Problem and Concepts. A general multiobjective optimization problem consisted of m objective functions and $(J + K)$ constraints, defined by N decision variables, is represented as follows:

$$\begin{aligned}
&\min/\max F(x) \\
&\quad = \{(f_1(x) + p_1), (f_2(x) + p_2), \ldots, (f_m(x) + p_m)\}, \\
&\qquad\qquad\qquad\qquad x \in \mathrm{DS}, \\
&\mathrm{DS} = \{x_n^L \le x_n \le x_n^L,\ n = 1, 2, \ldots, N\}\ , \\
&\mathrm{SS} = \Big\{x : g_j(x) \le 0,\ h_k(x) = 0, \\
&\qquad j = 1, 2, \ldots, J,\ k = 1, 2, \ldots, K\Big\}
\end{aligned} \tag{1}$$

X bounded by an upper and lower value, x_n^U and x_n^L are used to represent a decision variable set defined in decision variable space (DS) and computation of both objective functions f and constrains $g_j(x)$ and $h_k(x)$ in a solution space (SS). In order to explore the optimal solutions (designations) located in feasible region (FR) which contains the unpenalized solutions of SS, the obtained solutions are penalized when they do not satisfy the constraint conditions. Then, the penalized values denoted by p are included into their related objective functions f.

At each run of an evolutionary optimization algorithm, a random solutions set is obtained. Some of them are Nondominated solutions (none is better for all objectives) and referred to as "pareto solution" defined in a concept named as domination [9]. Thus, the pareto solutions are used to form "pareto front" which determines bounds of Nondominated solutions.

2.2. First Steps in MOAs. After introduction of the evolutionary mechanism to the multi-objective optimization problem, the development of new multi-objective approaches has been accelerated [4]. Primary one of these approaches is Nondominated Sorting Genetic Algorithm (NSGA) proposed by Srinivas and Deb [5]. NSGA determines the Nondominated solutions according to ranks of their reproductive potentials.

Although pareto-ranking procedure gives a guarantee for transmission of elite individuals to next generations, an excessive repetition of ranking procedure causes to lose promising genetic material due to the genetically distortion of migrated data. In order to diminish this negative effect, Niched Pareto Genetic Algorithm (NPGA) that determined the Nondominated solutions by tournament selection method was suggested [6]. Afterwards, Fonseca and Fleming [7] suggested a penalization process that generated the promising pareto solutions considering their crowding densities.

Using an external archive to store Nondominated solutions leads to an increase in the capabilities of multi-objective optimization tools, such as in an evolutionary search proposed by Zitzler and Thiele, called Strength Pareto Evolutionary Algorithm (SPEA) [10]. The members of external archive are chosen according to their closeness to pareto front. However, enlargement of the external archive makes the convergence speed of its evolutionary search to be poor due to a decrease in its selection pressure. In order to deal with this difficulty, Knowles and Corne [11] suggested a grid system, called Pareto Archived Evolutionary Strategy (PAES) to compute the optimization-related procedures.

Hence, distributing the entire population to this grid system by an adaptive mapping process, which of each node was used to represent an individual, makes it easier to maintain the diversity in pareto set.

2.3. An Overview of MOAs Applied in Field of Structural Engineering. Although MOAs mentioned above are successful for a solution space represented by design variable of continuous type, they fail to explore optimal designations in nonconcave and discontinuous solution space of structural design problems represented by design variables of discrete type. Hence, the preliminary studies in the field of structural engineering with multiple objectives were developed using weighting [12], goal programming [13, 14], and modified game theory methods [15]. Sunar and Kahraman [16] compared the computational performances of these algorithms considering optimal designations of a space truss with 25 bars and a satellite system and showed that modified game theory and goal programming were superior to weighting approach. Although it was reported that the weighting approach failed to explore Nondominated solutions on nonconvex parts of pareto front [17–19], it has been improved due to its easy adaptable mechanism. One of these attempts was based on a systematic alteration of objective function weights [20]. This adaptive approach was applied to design optimization of a truss problem with 3 bars and achieved to obtain a well-distributed pareto set in a nonconcave solution space.

Real-world engineering structures are represented by a large number of discrete design variables. Hence, the evolutionary search is easily misguided due to an increase in the computational effort. Therefore, new optimization algorithms inspired by some biological events, such as particle swarm, differential evolution [21], artificial immune system [22], ant colony [23], and some other evolutionary algorithms, such as microgenetic algorithm [24] have been utilized to solve optimization problems with multiple objectives.

Janga and Nagesh proposed an evolutionary technique, called elitist-mutated particle swarm optimization and applied to three test problems: design optimizations of two-bar truss, I-beam, and welded beam [25].

Cooperate and coevolutionary strategies were introduced to the evolutionary search mechanism to increase diversity within the set of Nondominated solutions stored [26]. For this purpose, chromosomes divided into different species are recombined and evolved to create a pareto set. However, the number of chromosomes chosen may exceed their predetermined number. In order to deal with this difficulty, the exceeded number of chromosomes is reduced according to the qualities of their crowding distances and redistributed using an elitism strategy. The fundamentals of NSGA [5], Niched Pareto Genetic Algorithm (NPGA) [27, 28], and Controlled Elitist Nondominated Genetic Algorithm (CNSGA) [5] were constituted on this approach. The proposed evolutionary approach, which of main evolutionary operations has similarities to the optimization algorithms named NSGA, NPGA, and CNSGA, were utilized for topology optimization of 2D heat transfer structures. It was demonstrated that using a decreased size of species increased the computational performance of the proposed optimization procedure.

The other promising approaches were developed as hybridizing these methods with each other. One of substantial attempts is the integration of neural network and fuzzy systems to provide a control mechanism for an evolutionary mechanism [29]. While a neural network is utilized to predict an individual with higher quality, operator parameters of evolutionary algorithm are updated according to the rules of fuzzy logic. This hybrid system was applied for design optimization of several composite beams with three layers, piezoelectric bimorph beam, a truss structure, and airplane wing and displayed to obtain more converged optimal designations comparing to a pure and independent usage of each algorithms without any hybrid implementation.

3. Introduction of MOAs, NSGAII, SPEA II, PESA II, and AbYSS for Design Optimization of Grillage Systems Utilizing Multiple Objectives

Although it is displayed that the evolutionary algorithms have been successfully utilized as optimization tools, some computational bottlenecks cause to obtain a poor-distributed pareto front. In order to increase their ability in generation of promising designations for a diverse pareto front, the conventional MOAs have been improved and/or developed. The promising versions are NSGA II, SPEA II, PESA II, and AbYSS. In this study, these improved or developed MOAs, are utilized for the optimal designations of grillage systems noting that the design optimization of grillage systems was carried out using a single objective by up to now [30–32] and a displacement-based matrix analysis approach [33]. In order to execute their optimization procedures, JMETAL coded in a programming language Java is employed [34]. Both JMETAL and the proposed four MOAs are introduced in the following subsections.

A Brief Introduction of JMETAL. JMETAL coded in a platform of object-oriented Java is used as an optimization tool to solve the multi-objective optimization problems [34]. It contains a number of classes which represent the building blocks of various multiobjective algorithms. However, their basic evolutionary-related elements are the same. Therefore, the architecture of JMETAL is constituted on a simple but an interdependently higher framework. JMETAL is an open source project. The computational procedures of various MOAs including the ones employed in this study are extensively documented in [34]. Therefore, the description of its base classes is not presented. Instead, the computational order of the preliminary classes that contain the fundamental parameters is briefly depicted by the pseudocodes. Whereas the class names are presented by use of a mark " ", their related parameters are defined by use of italic characters.

In general, JMETAL contains six packages, named "base, experiments, metaheuristics, problems, quality indicator and util". While the package of "experiments" includes

```
Initialize population (population_size)
evaluate population, evolution ++
while evolution  <max_evolution {
        if evolution <max_evolution {
        Offspring =mutation(crossover(selection(population)))
        evaluate offspring, evolution ++}
front=ranking(population U offspring).getsubfront
population.clear
front=CrowdingDistanceAssignment(front)
population.add(front)
        if HV ≥ 0.98 * trueparetofronthypervolume {
        stop}}
front=Ranking(population).getsubfront
```

Algorithm 1: A pseudocode for NSGA II procedure.

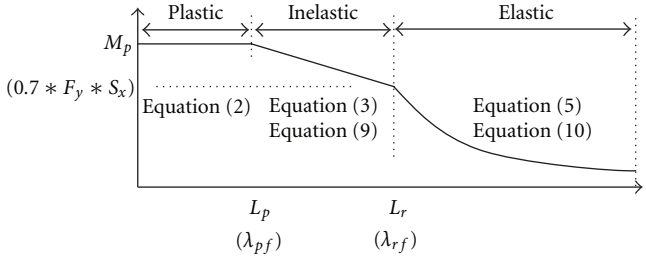

Figure 1: Nominal flexural strength as a function of "flange width-thickness ration of rolled I-shapes" and "unbraced length and moment gradient" (it corresponds to Figure C-F1.1 and C-F1.2.1 in the design manual of AISC-LRFD Ver.13).

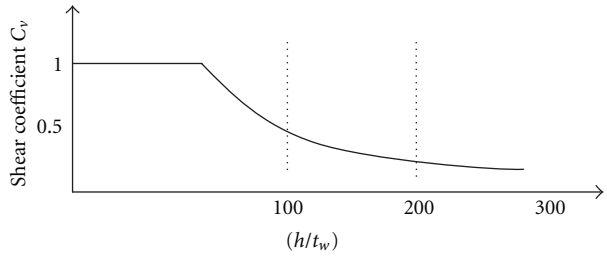

Figure 2: Shear coefficient C_v for F_y = 50 ksi and k_v = 5.0 (it corresponds to Figure C-G2.1 in the design manual of AISC-LRFD).

configurations of various metaheuristic procedures, such as AbYSS and NSGAII, their default configurations are located in the "settings" package. Design problems with various complexities are comprised in the "problems" package. The run of JMETAL firstly begins by execution of a purposed metaheuristic class, such as AbYSS.Java, located in the "experiments" package. This class invokes the experiment class which is responsible for activation of proposed metaheuristic algorithm. The purposed metaheuristic class invokes a class of design problem to be solved. Basic computation processes, named "evaluate () and evaluateconstaint ()," are carried out in this class, named design problem. Due to the use of binary coding scheme for the evolutionary computations, generated individuals can exceed the predefined upper bounds of design variables. In order to deal with inappropriate binary strings, the purposed meta-heuristic class named AbYSS.Java, and its related subclasses are extended by including a new class named "repairing mechanism" which is responsible to correct the decoded values of binary strings according to the limits of design variables.

3.1. Nondominated Sorting Genetic Algorithm II, NSGA II. NSGA was firstly designed by Srinivas and Deb [5]. The evolutionary computation of NSGA is managed by classified "population size" individuals. Classification process begins firstly ranking the population in order to determine Non-dominated individuals. Then, fitness values of individuals are shared considering their niching measures. The individuals with shared fitness values are selected by use of a selection method, called "stochastic universal sampling" and regenerated using mutation operator with a probability *mutation_probablity* and combination operator with a probability *crossover_probablity* until completing a predetermined evolution number *max_evolution*. The enhanced version of NSGA, NSGA II (see pseudocode in Algorithm 1) was developed to increase diversity among individuals [35, 36]. Although NSGA II utilizes the evolutionary operators for generation of individuals as in the computational procedure of NSGA, the generated individuals stored in an archive with *population_size* individuals are used to obtain a pareto front considering crowding distances of individuals. Furthermore, a hypercube, which is formed by use of the Nondominated individuals, is utilized to compute a hypervolume.

3.2. Improved Strength Pareto Evolutionary Algorithm, SPEA II. The primary version of SPEA approach was firstly suggested by Zitzler and Thiele [10]. Its evolutionary processes are managed by two populations. While one of these populations, called regular population is utilized to generate offspring, other population, called an archive with *archive_size* individuals is employed to preserve the evolutionary information of pareto front. In the beginning of evolutionary process, the archive is empty and filled by promising individuals. The exceed number of individuals are reduced giving a higher chance to the individuals of

```
initiliaze solutionSet(population_size), solution (population_size)
initiliaze archive (archive_size)
evaluate solution, evolution ++
solutionSet.add(solution)
while evolution<max_evolution {
        spea=Spea2Fitness(solutionsSet U archive)
        spea.FitnessAssignmanet
        archive=spea.enviromantalSelection(archive_size)
                if evolution <max_evolution {
                offspring=mutation(crossover(selection(archive)))
                evaluate offspring, evolution ++}
        solutionSet.add(offspring)}
front=Ranking(archive).getsubfront
```

Algorithm 2: A pseudocode for SPEA II procedure.

```
initialize archive = AdaptiveGridArchive (archive_size, bisections)
initialize solutionSet (population_size)
initialize solution (population_size)
solution = PESAIIselection (solution)
evaluate solution, evolution ++
solutionSet.add(solution)
archive.add(solutionSet)
solutionSet.clear
while evolution < max_evolution {
        offspring=mutation(crossover(selection(archive)))
        evaluate offspring, evolution ++
        solutionSet.add(offspring)
        archive.add(solutionSet)
        solutionSet.clear}
```

Algorithm 3: A pseudocode for PESA II procedure.

archive. For this purpose, a clustering technique which is based on an assignment of strength value to the individuals and an assessment of these individuals according to their strength values is utilized to discard the related individuals. However, a decrease in variation among individuals of population causes to increase the randomness in the evolutionary search and hence decrease the accuracy degree of density estimation, which is utilized by clustering process [37]. This leads to vanishing of the promising solutions located on the pareto front. In order to deal with this negativity, SPEA II is developed. SPEA II estimates density of strength values using kth nearest neighbor method (see Algorithm 2). Furthermore, a new selection mechanism, called "environmental selection", is used to update the archive and to preserve promising solutions during truncation of archive.

3.3. Improved Pareto Envelope-Based Selection Algorithm (Region-Based Selection), PESA II. Pareto Envelope-Based Selection Algorithm (PESA) was firstly presented by Corne et al. [38]. Having similarities to basic features of SPEA II, PESA uses two populations for its evolutionary processes. However, in the estimation of strength-value density, PESA uses a measure called "sequence factor." An extended version of PESA, PESA II, utilizes hyperboxes which are obtained by dividing the entire search space into small ones (see Algorithm 3). Thus, the number of individuals contained in hyperboxes is used to determine a sequence factor. Following the determination of subregion numbers defined by *bisections*, the archive is created in the module named "AdaptiveGridArchive." A population called "solution" is initialized and evolved by the application of evolutionary operators until being completed a fixed evolution number. Although SPEA II was shown to be computationally faster than NSGA II and SPEA II, some complicating tasks, such as possibility of existing dominated individuals in any hyperboxes, keeping a fixed number of subregions throughout the evolutionary search, and so forth, must be overcome in order to obtain satisfactory optimal designations [39, 40].

3.4. Adaptive Scatter Search for Multiobjective Optimization, AbYSS. AbYSS can be categorized as an evolutionary-search-based optimization algorithm derived by use of principle features of NSGA II, PESA II, and SEPA II [41]. A pseudocode for ABYSS is presented in Algorithm 4. After initializing a population with *population_size* individuals, the population is firstly regenerated using grid-based search technique named "diversification generation." Then, the regenerated population is maintained by discarding the mutated individuals with poor qualities according to a dominance-based comparison test. This elimination process named "improvement" is inspired from NSGA II approach. Then, a search process named "reference update" is invoked to firstly construct a sub-population *RefSet2* with *Ref_Set_size*

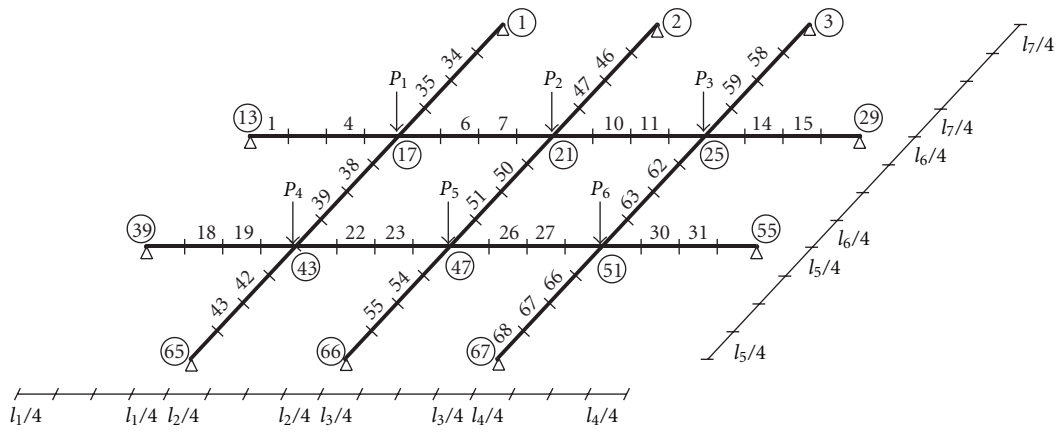

Figure 3: Geometry of 68-members grid structure including locations of point loads.

individuals from a sub-population RefSet1 with *Ref_Set2_size* individuals and then, update the sub-population RefSet2. The sub-population RefSet2 is built by the individuals of RefSet1 with minimum euclidian distance. After generation of reference sets, the Nondominated individuals extracted from the reference sets are stored in an external population called archive with *archive_size* individuals using density estimation of individuals. In this regard, the existence of individuals in a densest region is identified considering their niching measures. Its features of utilizing the niching measures and density estimation for the evolutionary search are inspired from adaptive grid method by PAES II and selection strategy by SPEA II, respectively.

4. Optimum Design of Grillage Systems

The proposed four MOAs are presented in the previous section. These MOAs are evaluated for the optimal designations of grillage systems in this study. For this purpose, the objective functions, their related constraints, and structural analysis procedures are coded in Java. In this regard, the design requirements used in constraints and design optimization procedure are introduced in Sections 4.1 and 4.2.

4.1. Design Requirements of Grillage Systems according to LRFD-AISC Ver.13. Grillage systems comprise a number of lateral braced beams. If the beams loaded in plane of lateral system have no sufficient lateral stiffness, then they are buckled out of plane of loading. This case is called lateral-torsional buckling. The lateral-torsional buckling strength varies depending on the unbraced length and compactness of beam plays an important role in the load carrying capacity of beam. If a compact beam determined according to its web and flange dimensions has a sufficient unbraced length, then nominal flexural strength is calculated in an elastic domain, otherwise an inelastic one. In the inelastic case, a short and unbraced beam length causes to yield its outer fibers before attaining elastic buckling load. The formulation of nominal flexural strength M_n that is managed by limit states of yielding, lateral torsional, and flange local buckling is presented in the following part as defined in AISC-LRFD Ver.13 (see Figure 1). For simplicity, two distinct figures used to depict the lateral-torsional and flange local buckling depicted in AISC-LRFD Ver.13 is coarsely combined, but equation numbers corresponding to formulations for limit states are presented in a separate parenthesis.

The limit states of yielding of beam cross-section are written as

$$M_n = M_p = F_y * Z_x. \tag{2}$$

In elastic and inelastic domains, two unbraced lengths L_p and L_r are used to determine the compactness of sections manage the strength of lateral-torsional buckling. Nominal-flexural strength M_n is computed as follows.

For inelastic-torsional buckling limited by $L_p < L_b < L_r$,

$$M_n = C_b * \left[M_p - \left(M_p - 0.7 * F_y * S_x \right) * \left(\frac{\left(L_b - L_p \right)}{\left(L_r - L_p \right)} \right) \right], \tag{3}$$

where,

$$L_p = 1.76 * r_y * \sqrt{\frac{E}{F_y}},$$

$$L_r = 1.95 * r_{ts} * \frac{E}{\left(0.7 * F_y \right)} \sqrt{\frac{J_c}{(S_x * h_0)}} * \sqrt{1 + \sqrt{1 + 6.76 * \left(\frac{\left(0.7 * F_y \right)}{E} * \frac{(S_x * h_0)}{J_c} \right)^2}}. \tag{4}$$

For elastic-torsional buckling occurred in a segment limited by $L_r < L_b$ (see Figure 1),

$$M_n = F_{cr} * S_x, \tag{5}$$

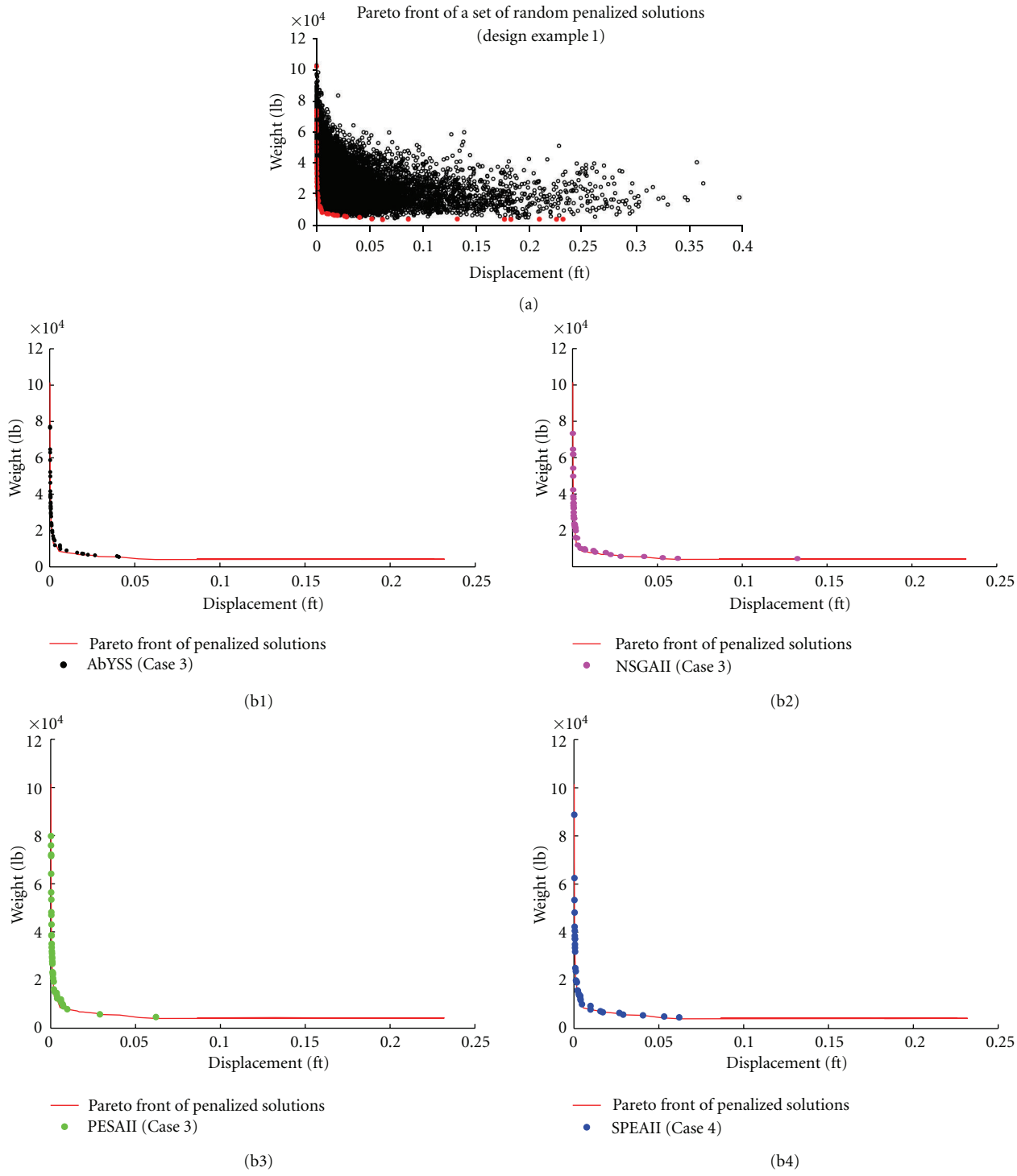

FIGURE 4: Pareto fronts of a set of random nondominated solutions obtained by use of an increased population size and evolution number (a) and AbYSS, NSGAII, PESAII, and SPEAII (b1)–(b4).

where,

$$F_{\text{cr}} = \frac{(C_b * \pi^2 * E)}{(L_b/r_{\text{ts}})^2} \sqrt{1 + 0.078 * \frac{J_c}{S_x * h_0} * \left(\frac{L_b}{r_{\text{ts}}}\right)^2}, \quad (6)$$

$$r_{\text{ts}}^2 = \frac{I_y * h_0}{2 * S_x}. \quad (7)$$

In (6), moment modification factor C_b is utilized to consider the effect of lower torsional buckling arisen from a

nonuniform distribution of moment. Therefore, associating with moment diagrams, it is computed as follows.

$$C_b = \frac{12.5 * M_{\max}}{2.5 * M_{\max} + 3 * M_A + 4 * M_B + 3 * M_C}. \quad (8)$$

The local buckling of flanges for noncompact section is governed by two parameters, λ_{pf}, λ_{rf}. Depending on these parameters, nominal-flexural strength M_n is computed as follows.

For inelastic-flange buckling occurred in a segment limited by $\lambda_{pf} < (b_f/2t_f) < \lambda_{rf}$,

$$M_n = \left[M_p - \left(M_p - 0.7 * F_y * S_x\right) * \left(\frac{\left(\lambda - \lambda_{pf}\right)}{\left(\lambda_{rf} - \lambda_{pf}\right)}\right)\right]. \quad (9)$$

For elastic-flange buckling occurred in a segment limited by $\lambda_{rf} < b_f/2t_f$,

$$M_n = \frac{(0.9 * E * k_c * S_x)}{\lambda^2}. \quad (10)$$

In addition, nominal-shear strength V_n is computed as follows (see the limit states of shear strength in Figure 2):

$$V_n = 0.6 * F_y * A_w * C_v, \quad (11)$$

where,

$$C_v = \begin{cases} 1.0 \quad \text{if } \left(\dfrac{h}{t_w}\right) \le 1.10 * \sqrt{k_v \dfrac{E}{F_y}}, \\ \dfrac{\left(1.10 * \sqrt{k_v * \left(E/F_y\right)}\right)}{(h/t_w)} \\ \quad \text{if } 1.10 * \sqrt{k_v \dfrac{E}{F_y}} \le \left(\dfrac{h}{t_w}\right) \le 137 * \sqrt{k_v \dfrac{E}{F_y}}, \\ \dfrac{(1.51 * E * k_v)}{(h/t_w)^2 * F_y} \\ \quad \text{if } \left(\dfrac{h}{t_w}\right) \ge 1.37 * \sqrt{k_v \dfrac{E}{F_y}}. \end{cases} \quad (12)$$

In (11), web-plate buckling coefficient k_v is equal to 5 for unstiffened webs with $(h/t_w < 260)$.

4.2. Design Procedure for Optimal Grillage Systems. In this work, a design problem of grillage system is represented by two objectives, entire weight of grillage system, and joint deflection, and expressed as follows:

$$\min W = \left(\sum_{k=1}^{m} (w * l)_k + p_1\right), \qquad \min d = \left(\max(d) + p_2\right),$$
$$(k = 1, \ldots, m,\ i = 1, \ldots, 12,\ j = 1, \ldots, n). \quad (13)$$

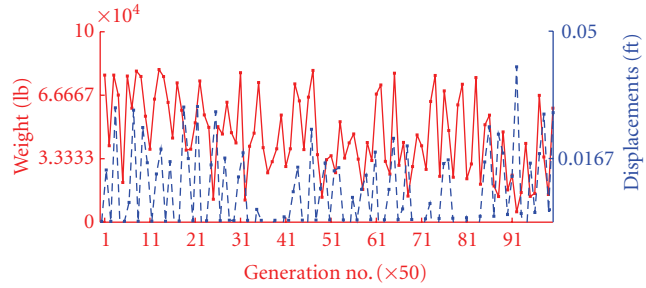

Figure 5: Convergence history obtained by AbYSS (Case 3).

Subject to

$$g_{1k} = \frac{M_u}{(\phi_b * M_n)} \quad (k = 1, \ldots, m), \quad (14)$$

$$g_{2k} = \frac{V_u}{(\phi_s * V_n)} \quad (k = 1, \ldots, m), \quad (15)$$

$$g_{3ij} = \frac{d}{d_{\max}} \quad (i = 1, \ldots, 12,\ j = 1, \ldots n), \quad (16)$$

$$p_1 = \left(\sum_{k=1}^{m} (g_{1k} + g_{2k})\right) * (r_0 * t)^{\varphi} * f \quad \{\text{if } g_{1k} \text{ or } g_{2k} \ge 1\ (k = 1, \ldots, m)\}, \quad (17)$$

$$p_2 = \left(\sum_{j=1}^{n} \sum_{i=1}^{12} g_{3ij}\right) * (r_0 * t)^{\varphi} * f \quad \left\{\text{if } g_{3ij} \ge 1\ (i = 1, \ldots, 12,\ j = 1, \ldots, n)\right\}. \quad (18)$$

The term W is total weight of all grid members and computed using w and l which are unit weight to be selected from W-sections list of LRFD-AISC Ver.13 and length of a grid member. While d is termed as a joint displacement corresponding to related degree of freedom which is denoted i, total numbers of joint and grid member are indicated by n and m. $d_{\max}$ is taken as (max span/300). In constraint inequalities, while displacements of joints are constrained by an upper limit $f_{\max}$, bending-moment strength of grid members M_u is limited by allowable nominal-moment strength M_n. Shear strength of grid members V_u is limited by allowable nominal-shear strength V_n (see V_n in (11)). In (14) and (15), ϕ_b and ϕ_s are resistance factors for moment and shear and taken as 0.9. Furthermore, it must be noted that M_n indicated in (14) manages total three strength requirements: yielding (2), flange-local buckling (9) and (10), and lateral-torsional buckling (3) and (5).

5. Search Methodology

Due to the fact that application problems are chosen from real-world engineering design problems with design variables of discrete type, a reliable and consistent search

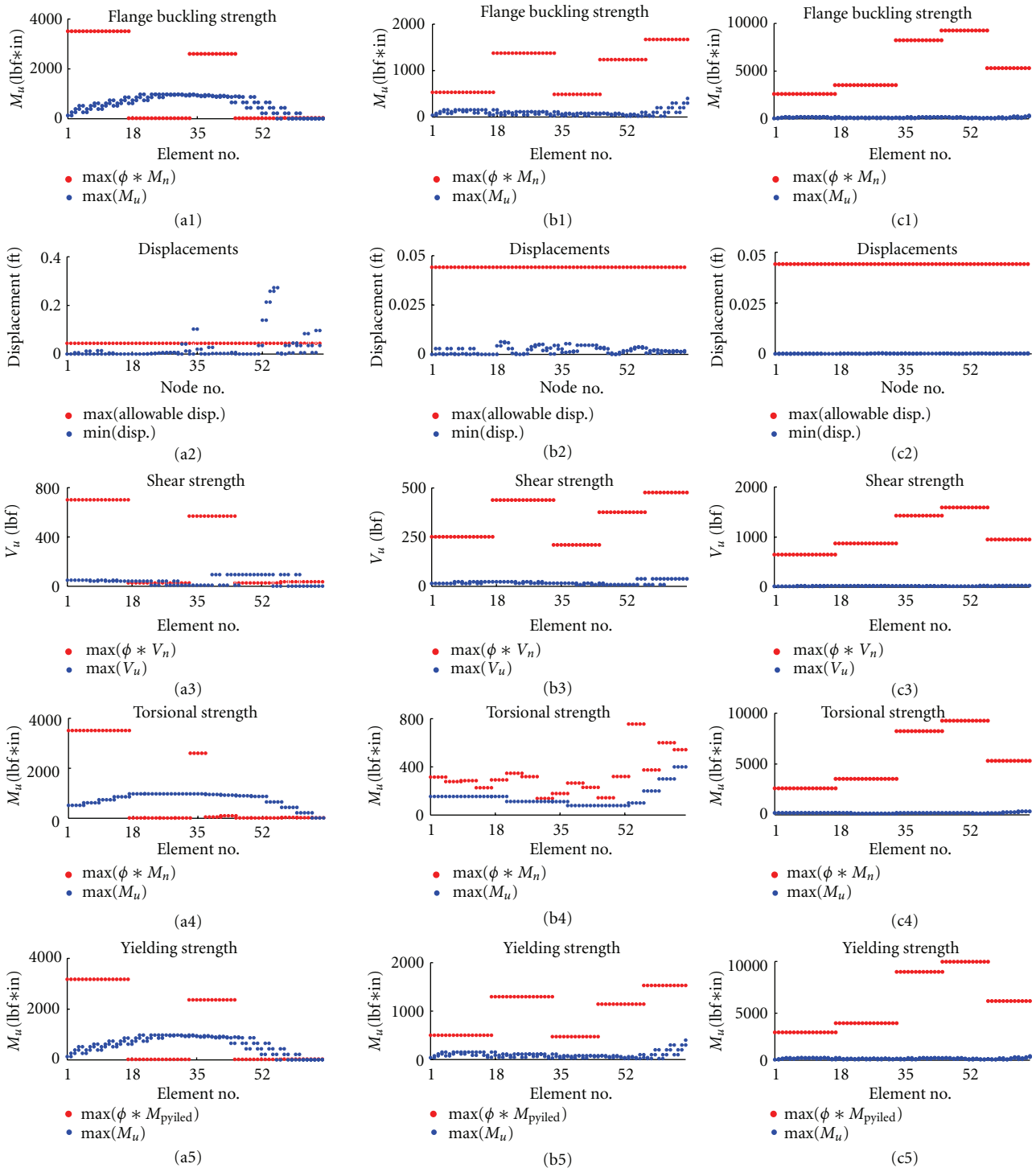

FIGURE 6: Strengths and displacements of random penalized solutions corresponding to minimum displacement (a1)–(a5), unpenalized solutions corresponding to maximum displacement (b1)–(b5), and maximum weight (c1)–(c5) (see Figure 5).

strategy must be established for an evaluation of proposed MOAs' search capabilities. After generating optimal designations, the computational performances of MOAs are assessed according to the closeness of these designations to a pareto front known beforehand thereby using a number of quality measuring metrics. Furthermore, accuracy of assessment of multiobjective optimization algorithms must be confirmed by outcomes of statistical tests. The other important difficulty is how to adopt a common methodology for a conventional mathematical model, which is performed its computational procedures by usage of design variables of continuous type. Therefore, a reasonable approach is

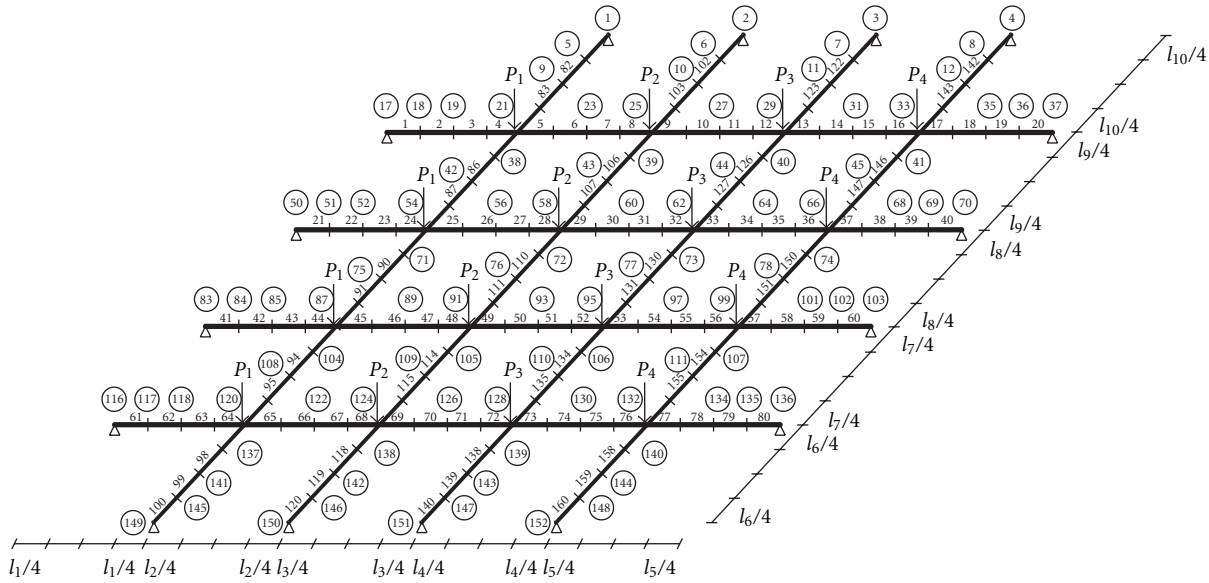

Figure 7: Geometry of 160-members grid structure including locations of point loads.

to obtain a pareto front by running current discrete optimization model in bigger and repeated generation numbers. In this regard, independent 10 runs of proposed MOAs are executed by use of both increased and decreased size of generation and population. Then, optimal designations obtained are utilized in computation of quality-measuring metrics, such as hyper volume and generational distance. Due to the nature of stochastic algorithms, a statistical test for analysis of these quality-measuring metrics computed must be performed with a certain level of confidence. Moreover, in order to decrease the effect of parameter values of evolutionary operators on MOAs' performance evaluation, various parameter combinations are also considered. Details about quality-measuring metrics and statistical tests employed for MOAs' performance assessment are presented in Sections 5.1 and 5.2.

5.1. Quality-Measuring Metrics. Differentiation in MOAs architecture prevents to lay down the different aspects of MOAs' performance. Therefore, quality indicators have a big impact on accurately evaluation of MOAs performance. In this study, three quality indicators, hyper volume ratio (Hv), inverted generational distance (IGD), and spread (S) are employed.

Hyper Volume Ratio. Hyper volume (HV) is an indicator which defines a volume covered by n Nondominated set of solutions included in a region bounded by a pareto front (see (17)). For this purpose, a reference point chosen among Nondominated solutions with worst objective is utilized in computation of hypercube of each Nondominated solutions,

$$\mathrm{HV} = \mathrm{volume}\left(\bigcup_{i=1}^{n} V_i \mid \mathrm{refpoint}\right). \tag{19}$$

Hyper volume ratio (HVR) is an indicator which shows a ratio of current hyper volume to the true hyper volume computed by use of true pareto front and nondominated solutions true pareto front (see (18)),

$$\mathrm{HVR} = \frac{\mathrm{HV}_{\mathrm{current}}}{\mathrm{HV}_{\mathrm{true}}}. \tag{20}$$

Higher values of HVR indicate a large coverage of Nondominated solutions in a solution space.

Inverted Generational Distance. Inverted generational distance (IGD) estimates the far of Nondominated solutions included in current pareto front generated by the proposed MOA, from those included in true pareto front (see (19)),

$$\mathrm{IGD} = \frac{\sqrt{\sum_{i=1}^{n} d_i^2}}{n}, \tag{21}$$

where n is number of Nondominated solutions found by proposed MOA and d_i is Euclidian distance between each of these and nearest member of true pareto front. A lower value of IGD indicates an increase in approximation of current pareto front obtained to the true pareto front in terms of convergence.

Spread. This quality metric abbreviated as (S) is used to measure an expanding spread exhibited by Nondominated solutions obtained and computed as

$$S = \frac{d_f + d_l + \sum_{i=1}^{N-1} \left| d_i - \overline{d} \right|}{d_f + d_l + (N-1) * \overline{d}}, \tag{22}$$

where d_i is Euclidian distance between consecutive Nondominated solutions, $\overline{d}$ is mean of these distances, and d_f and d_l are distances to extreme solutions of current pareto

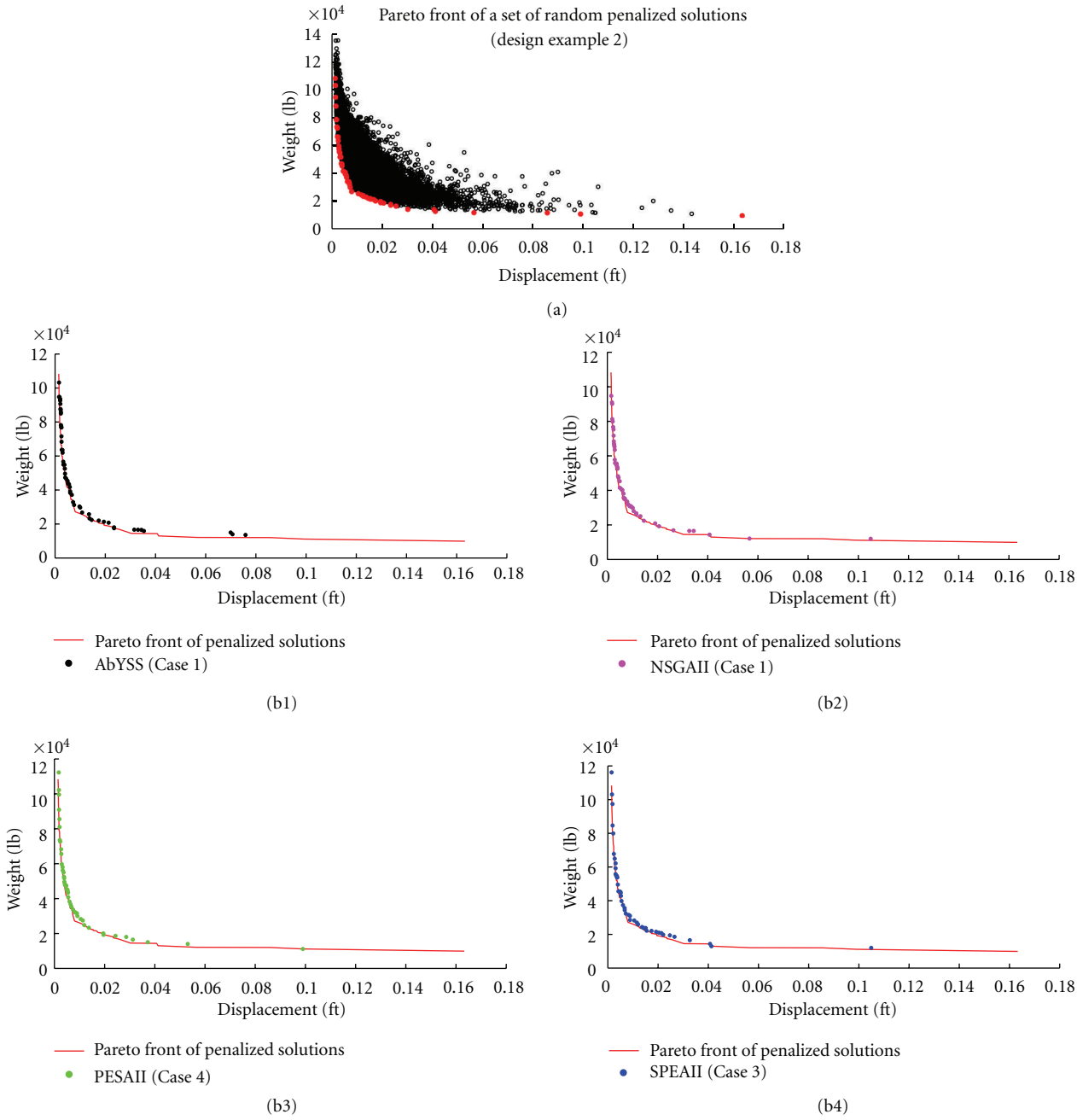

FIGURE 8: Pareto fronts of a set of random nondominated solutions obtained by use of an increased population size and evolution number (a) and AbYSS, NSGAII, PESAII, and SPEAII (b1)–(b4).

front. A lower S value points out a better distribution among Nondominated solutions. In other words, it is implied that Nondominated solutions are located in different positions.

5.2. Statistical Tests. The quality indicators mentioned above are utilized in comparison of MOAs' distribution qualities. Therefore, after computing means and standard deviations of quality indicators obtained by in the end of independent 10 executions, consistency of these results are checked through performing a statistical analysis in a certain level of confidence. If a probability value resulted from a statistical testing procedure satisfies a user-defined significance level, then it is said that distribution of current MOAs approximation set is acceptable.

Computational procedures of the statistical analysis are performed in MATLAB [42]. Firstly, lillie test is carried out to check quality indicator values for whether to be exhibited a normal distribution (if the null distribution is completely specified, then Kolmogorov-Smirnov test is more appropriate). Then, existence of a variance homogeneity is controlled through Levene' test. If homogeneity in the variance exists, Welch test is performed, otherwise Anova

Table 1: Cases used to represent the parameter combination for evolutionary operators of MOAs and their assigned values.

	NSGA II		SPEA II		PESA II		AbYSS	
Population size	50 and 100		50 and 100		50 and 100		50 and 100	
Evolution number	1,000 and 5,000		1,000 and 5,000		1,000 and 5,000		1,000 and 5,000	
Crossover probability	1.00^{1}	1.00^{5}	1.00^{1}	1.00^{5}	1.00^{1}	1.00^{5}	*1.00*^{1}	1.00^{5}
	0.25^{2}	0.25^{6}	0.25^{2}	0.25^{6}	0.25^{2}	0.25^{6}	*0.25*^{2}	0.25^{6}
	1.00^{3}	1.00^{7}	1.00^{3}	1.00^{7}	1.00^{3}	1.00^{7}	*1.00*^{3}	1.00^{7}
	0.25^{4}	0.25^{8}	0.25^{4}	0.25^{8}	0.25^{4}	0.25^{8}	*0.25*^{4}	0.25^{8}
Mutation probability	1.00^{1}	1.00^{5}	1.00^{1}	1.00^{5}	1.00^{1}	1.00^{5}	*1.00*^{1}	1.00^{5}
	0.25^{2}	0.25^{6}	0.25^{2}	0.25^{6}	0.25^{2}	0.25^{6}	*0.25*^{2}	0.25^{6}
	0.25^{3}	0.25^{7}	0.25^{3}	0.25^{7}	0.25^{3}	0.25^{7}	*0.25*^{3}	0.25^{7}
	1.00^{4}	1.00^{8}	1.00^{4}	1.00^{8}	1.00^{4}	1.00^{8}	*1.00*^{4}	1.00^{8}
Crossover Distribution Index	30^{1}	15^{5}	30^{1}	15^{5}	30^{1}	15^{5}	*30*^{1}	15^{5}
	8^{2}	4^{6}	8^{2}	4^{6}	8^{2}	4^{6}	*8*^{2}	4^{6}
	30^{3}	15^{7}	30^{3}	15^{7}	30^{3}	15^{7}	*30*^{3}	15^{7}
	8^{4}	4^{8}	8^{4}	4^{8}	8^{4}	4^{8}	*8*^{4}	4^{8}
Mutation Distribution Index	30^{1}	15^{5}	30^{1}	15^{5}	30^{1}	15^{5}	*30*^{1}	15^{5}
	8^{2}	4^{6}	8^{2}	4^{6}	8^{2}	4^{6}	*8*^{2}	4^{6}
	8^{3}	4^{7}	8^{3}	4^{7}	8^{3}	4^{7}	*8*^{3}	4^{7}
	30^{4}	15^{8}	30^{4}	15^{8}	30^{4}	15^{8}	*30*^{4}	15^{8}
Reference set I	—		—	—	—	—	*20*	20
Reference set II	—		—	—	—	—	*20*	20
Archive size	—		10	20	40	20	*40*	40
Bisection II	—		—	—	10	5	—	—

test. In order to compare the statistical outputs acquired from different algorithms, a post hoc testing is performed through "multicompare" function coded in MATLAB.

6. Discussion of Results

It is known that the computational performances of MOAs vary depending on the values of their interacting parameters. Therefore, in order to provide an accurate evaluation for their computational performances, some combination sets of parameter values are chosen. Due to a variety on the operator parameters of MOAs, various parameter combinations and the assigned values for their evolutionary operators are summarized in Table 1. The combination numbers (C. No.) are denoted by superscripts attached to related parameter values. In order to provide unbiased competition for the performance evaluation of MOAs employed, the parameter values of evolutionary operators are kept for each MOA. In this regard, the parameter combinations are sorted into two main groups denoted by numbers (1–4) and (5–8). Furthermore, each of main groups contains both upper and lower value sets of mutation and crossover distribution indexes in order to provide an intensive mutation or crossover effect for evolutionary search. For example, in first case of AbYSS (shown by italic characters in Table 1), Crossover and Mutation Probability values are 1.00 and 1.00; the values of Crossover and Mutation Distribution Indexes are 30 and 30; the values of Reference set I–II and archive size are 20, 20, and 40. Hence, reproducibility of related MOAs by use of these parameters is ensured. The detailed descriptions of these parameters are found in Section 3.

The penalty-related parameters used by penalty functions of weight and displacement are taken as $r_0 = 0.05$ and 0.005, $\varphi = 3$ and 2, and $f = 2$ and 1 for P_1 and P_2 (see (17) and (18)), respectively.

Using these different parameter combinations, an optimal design of grillage systems is carried out by four MOAs, NSGA II, SPEA II, PESA II, and AbYSS according to optimum design procedure mentioned previously. The yield stress, elastic modulus, and shear modulus of steel material used to construct the grillage system are taken as 50 ksi (345 MPa), 29,000 ksi (200 MPa), and 14,500 ksi (100 MPa). Cross-sectional properties of grid members are chosen from a discrete set with 274 W-sections. Sequence number of each cross-sections included in this profile list database is the same as given in LRFD-AISC Ver.13 and contains all sectional properties (such as area, inertia moments in all directions). Design variables are represented by binary strings. Thus, a binary length of $l = 9$ with $2^9 = 512$ possible gene combinations will be adequate to represent 274 ready sections. Profile list database, finite element attributes of design examples and a structural analysis formulation for the grillage system are coded in Java in order to appropriately compile with the optimization tool named JMETAL. In this regard, a user-defined input data coded in Java Language and related parts are presented for the design optimization of example 1 by utilizing AbYSS algorithm-based optimizer (see Algorithm 5). Details about class names and their related packages in Algorithm 4 are given in Section 3.

```
initialize solution (population_size)
solution=divesificationGeneration(solution)
evaluate solution, evolution ++
solution=improvement(solution)
solutionSet.add(solution)
while evolution < max_evolution {
// building and insertion of individuals RefSet1 and RefSet2
referenceUpdate(true)
newsolution=subsetGeneration
            while newsolution > 0 {
// update archive and reference sets using RefSet1 and RefSet2
referenceUpdate(false) }
                  if evolution < max_evolution {
            solutionSet.clear
            solution =RefSet1 (ref_set1_size)
            solution=improvement(solution)
            evaluate solution, evolution ++
            solutionSet.add(solution)
            RefSet1.clear
            RefSet2.clear
      // compute the crowding distance assignment of achieve
      //individuals. Then, after sorting the archive, use them to
      //create solutionSet with "insert" individuals
            insert=populationSize/2
            if insert > (archiveSize), insert= archiveSize
            if insert > (populationSize/2 – size(solutionSet)),
insert=(populationSize/2 – size(solutionSet))
            solutionSet.add (archive(insert))
      // complete randomly the remaining individuals of solutionSet
                  while size(solutionSet) < populationSize/2 {
            solution=divesificationGeneration(solution)
            evaluate solution, evolution ++
            solution=improvement(solution)
            solutionSet.add(solution) } } }
```

Algorithm 4: A pseudocode for AbYSS procedure.

Table 2: Values of measurement quantities obtained by "Eval. Number = 1,000" and "Pop. Size = 50" for design example 1.

C. no.	IGD				HV				Spread			
	AbYSS	NSGAII	PESAII	SPEAII	AbYSS	NSGAII	PESAII	SPEAII	AbYSS	NSGAII	PESAII	SPEAII
	Means											
1	0.1869	0.2575	0.1299	0.1067	0.5402	0.2284	0.7833	0.6032	**0.9089**	0.9995	0.9575	0.9875
2	0.2760	0.2543	0.1622	0.0844	0.6963	*0.8968*	0.1139	0.5999	0.9624	0.9810	0.9993	0.9737
3	0.1626	0.2435	0.1656	0.2599	0.5197	0.2754	0.8486	0.4484	0.9639	0.9562	*0.9359*	0.9723
4	0.1190	0.1966	0.2630	0.1818	0.8900	0.2818	0.4662	0.5138	0.9689	0.9790	0.9621	0.9852
5	**0.0358**	0.2511	0.0838	0.2638	0.3302	0.8801	0.3257	0.4077	0.9541	0.9508	0.9403	0.9922
6	0.2551	*0.0428*	0.2290	0.1455	0.2297	0.4443	0.6302	0.1080	0.9150	0.9917	0.9912	0.9954
7	0.1386	0.0759	0.1524	*0.0459*	*0.9045*	0.9045	*0.8787*	0.9045	0.9636	*0.9501*	0.9563	*0.9458*
8	0.1493	0.0540	*0.0301*	0.1450	0.3109	0.6033	0.5799	**0.9206**	0.9173	0.9883	0.9635	0.9620
	Standard deviations corresponding to best means and assessment of significance levels according to statistical tests											
	0.0018	0.0011	0.0051	0.0019	0.0022	0.0048	0.0064	0.0013	0.0051	0.0109	0.0103	0.0066
		(−)				(−)				(−)		

Design examples of real-world engineering structures are presented in an order of increasing size of their elements and joints. In order to display the change in the strength of grid members, both penalized and unpenalized optimal results corresponding to its maximum joint displacement or weight of grid structure are presented considering the joint and member numbers. Furthermore, convergence history obtained in the end of a complete evolutionary search is also presented. In order to provide an easier visualization for both weight and displacement values, the weight and displacement values are displayed for each of 100 equal segments obtained by a division of the maximum evolution number. Thus, the optimal designation located in one of these segments is easily determined.

```
public class AbYSSstudy extends Experiment {
...
public void algorithmSettings(Problem problem, int problemIndex) {
...
        parameters [0].setProperty("POPULATION_SIZE", "50");
        parameters [0].setProperty("MAX_EVOLUTIONS", "500");
        parameters [0].setProperty("REF_SET1_SIZE", "20");
        parameters [0].setProperty("REF_SET2_SIZE", "20");
        parameters [0].setProperty("ARCHIVE_SIZE", "40");
        parameters [0].setProperty("CROSSOVER_PROBABILITY",
"1.00");
        parameters [0].setProperty("MUTATION_PROBABILITY",
"1.00");
        parameters [0].setProperty("IMPROVEMENT_ROUNDS", "1");
...                                                          }
public static void main(String[] args) throws JMException,
IOException        {
...
    exp.experimentName_ = "AbYSSstudy";
    exp.algorithmNameList_ =newString                                  []
{"AbYSSa","AbYSSb","AbYSSc","AbYSSd","AbYSSe","AbYSSf","AbYS
Sg","AbYSSh","AbYSSi","AbYSSl","AbYSSm","AbYSSn","AbYSSo","A
bYSSp","AbYSSr","AbYSSs"};
    exp.problemList_ = new String[]{"example1"};
    exp.paretoFrontFile_ = new String[]{"example1.pf" };
    exp.indicatorList_ = new String[]{"HV", "SPREAD", "IGD",
"EPSILON"};
...
    exp.independentRuns_ = 10;            }}
public class example1 extends Problem {
    public example1(String solutionType) {
        numberOfVariables_ = 5;
        numberOfObjectives_ = 2;
        numberOfConstraints_ = 5;
        problemName_ = "example1";
        lowerLimit_ = new double[numberOfVariables_];
        upperLimit_ = new double[numberOfVariables_];
        lowerLimit_[0] = 1;
        lowerLimit_[1] = 1;
        upperLimit_[0] = 274;
        upperLimit_[1] = 274;
        variableType_ = new VariableType_[numberOfVariables_];
        length_        = new int[numberOfVariables_];
        length_ = new int[numberOfVariables_];
        solutionType        _        = Enum.valueOf(VariableType_.class,
    "SolutionType");
        for (int var = 0; var < numberOfVariables_; var ++){
        variableType_[var]        =        Enum.valueOf(VariableType_.class,
    solutionType);
        length_[var]        = numberOfBits;
        }
                                                    }
    public example1 (){
    }
    public void evaluate(Solution solution) throws JMException {
    ...              }
    public void evaluateConstraints(Solution solution) throws
    JMException {
    ...        }
```

Algorithm 5: An example input for AbYSS algorithm coded in Java.

6.1. Design Example 1: A Grid System with 4 and 3 Bays. This simple grillage system depicted in Figure 3 has four longitudinal and three lateral bays. Grid members of grillage system in x and y directions are linked into two separate groups: grid members (1–16) as design variable 1, grid members (17–32) as design variable 2, grid members (33–44) as design variable 3, grid members (45–56) as design variable 4, grid members (57–68) as design variable 5. Lengths of spans are l_1 = 10.500 ft (3.2004 m), l_2 = 11.500 ft (3.5052 m), l_3 = 12.000 ft (3.6576 m), l_4 = 9.250 ft (3.6576 m), l_5 = 13.250 ft (4.0386 m), l_6 = 12.500 ft (3.81 m), and l_7 = 10.000 ft (3.048 m). Magnitudes of loads are taken as 17.9847 kipf (80.00 kN) for P_1 and P_4, 20.2328 kipf (90.00 kN) for P_2 and P_5, 17.9847 kipf (80.00 kN) for P_2

Table 3: Values of measurement quantities obtained by "Eval. Number = 5,000" and "Pop. Size = 100" for design example 1.

C. no.	IGD				HV				Spread			
	AbYSS	NSGAII	PESAII	SPEAII	AbYSS	NSGAII	PESAII	SPEAII	AbYSS	NSGAII	PESAII	SPEAII
	Means											
1	0.0452	0.0382	0.0278	0.0435	0.9280	0.9521	0.9352	0.9029	0.8147	0.9293	0.9049	0.9203
2	0.0304	0.0324	0.0309	0.0274	0.9356	0.9106	0.9467	0.9490	0.9058	0.9172	0.9289	0.8819
3	*0.0246*	0.0443	0.0393	0.0346	**0.9863**	*0.9789*	*0.9849*	0.9414	**0.8067**	*0.8827*	*0.8683*	0.8555
4	0.0261	*0.0286*	*0.0247*	**0.0135**	0.9117	0.9079	0.9540	*0.9862*	0.9157	0.9106	0.9133	*0.8469*
5	0.0247	0.0418	0.0336	0.0442	0.9684	0.9013	0.9577	0.9145	0.8491	0.9027	0.9037	0.8797
6	0.0430	0.0388	0.0439	0.0160	0.9652	0.9160	0.9203	0.9715	0.8235	0.9001	0.8909	0.8754
7	0.0250	0.0316	0.0356	0.0419	0.9408	0.9140	0.9574	0.9196	0.8909	0.9294	0.9047	0.9160
8	0.0423	0.0299	0.0402	0.0415	0.9724	0.9668	0.9738	0.9141	0.8407	0.9234	0.8865	0.9174
	Standard deviations corresponding to best means and assessment of significance levels according to statistical tests											
	0.0011	0.0018	0.0045	0.0008	0.0024	0.0034	0.0048	0.0012	0.0028	0.0047	0.0084	0.0053
			(+)				(+)				(+)	

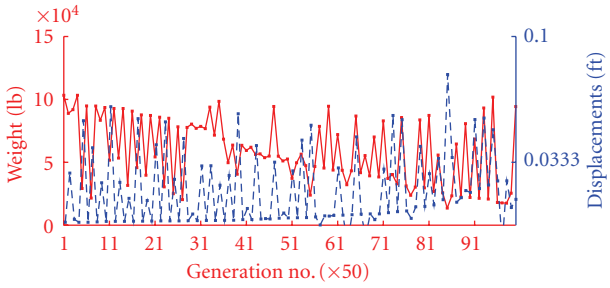

Figure 9: Convergence history obtained by AbYSS (Case 1).

and P_5, 15.7366 kipf (70.00 kN) for P_3, and 16.8606 kipf (75.00 kN) for P_6. The value of allowable displacement is constrained as (13.25/300 = 0.0441 ft; 13.4416 mm).

The pareto fronts of a set of random Nondominated solutions obtained by both use of an increased population size and evolution number and AbYSS, NSGAII, PESAII, and SPEAII are depicted in Figures 4(a) and 4(b1)–4(b4). The means of quality indicator values, standard deviations values corresponding to best means, and assessment of significance levels according to statistical tests are presented in Tables 2 and 3. Considering Tables 2 and 3, an increase in the evolution number and population size leads to an improvement in the values of quality indicator, in other words, an increase in the convergence degree of optimal designations. According to assessment of statistical analysis results corresponding to the lower evolution number and population size, it is clear that there is not a statistical confidence among proposed MOAs. The best values of quality indicators are obtained by AbYSS. SPEAII and PESAII exhibits better computational performance compared to NSGAII. It is also observed that an increase in the evolution number and population size forces MOAs to use higher values of operator parameter for improvement of their optimal designation qualities. This result is confirmed by examining the values of quality indicators with bold and italic characters. These higher quality indicator values are obtained by Cases 1–4, which indicate a usage of lower evolution number and population size and Cases 5–8, which indicate a usage of higher evolution number and population size. Considering the best spread values, the pareto fronts obtained by four MOAs employed are compared with both each other and the pareto front obtained by use of higher population size and evolution number (Figures 4(b1)–4(b4)). The convergence history of the optimizer AbYSS (Case 3) with the best spread value 0.8067 is presented in Figure 5 with two axes. A designation with (weight = 5446.1415 lb (2470.3282 kg) and displacement = 0.0406 ft (12.3748 mm)) is obtained in a generation of no. = 4638 located in a segment of no. 92 with an interval ($90 \times 50 = 4500$ and $100 \times 50 = 5000$).

The strength values of grid members are displayed considering penalized designation corresponding to a maximum displacement (weight = 18128.2500 lb (8222.835 kg) and displacement = 0.3977 ft (121.2189 mm); see Figures 6(a1)–6(a5)) and unpenalized designations corresponding to a maximum displacement (weight = 17095.5000 lb (7754.3883 kg) and displacement = 0.0068 ft (2.0721 mm)) and a maximum weight (weight = 74672.5000 lb (33870.8762 kg) and displacement = 0.0002 ft (0.0609 mm); see Figures 6(b1)–6(b5) and 6(c1)–6(c5)). Whereas the penalized designation corresponding to the maximum displacement contains a W-section set (W30×292, W6×12, W27×235, W6×12, and W8×15), the unpenalized designations corresponding to the maximum displacement and weight are represented by W-section sets (W24×68, W30×124, W27×129, and W30×148) and (W14×370, W14×455, W36×529, W36×652, and W36×361), respectively. The most critical strength values of penalized designation satisfied none of the constraints is obtained by both torsional and flange buckling-related constraints (see Figures 6(a1)–6(a5)). Examining the strength values depicted in Figures 6(b1)–6(b5) and 6(c1)–6(c5), limit state values of unpenalized designations corresponding to the maximum weight are higher than one corresponding to the maximum displacement due to a usage

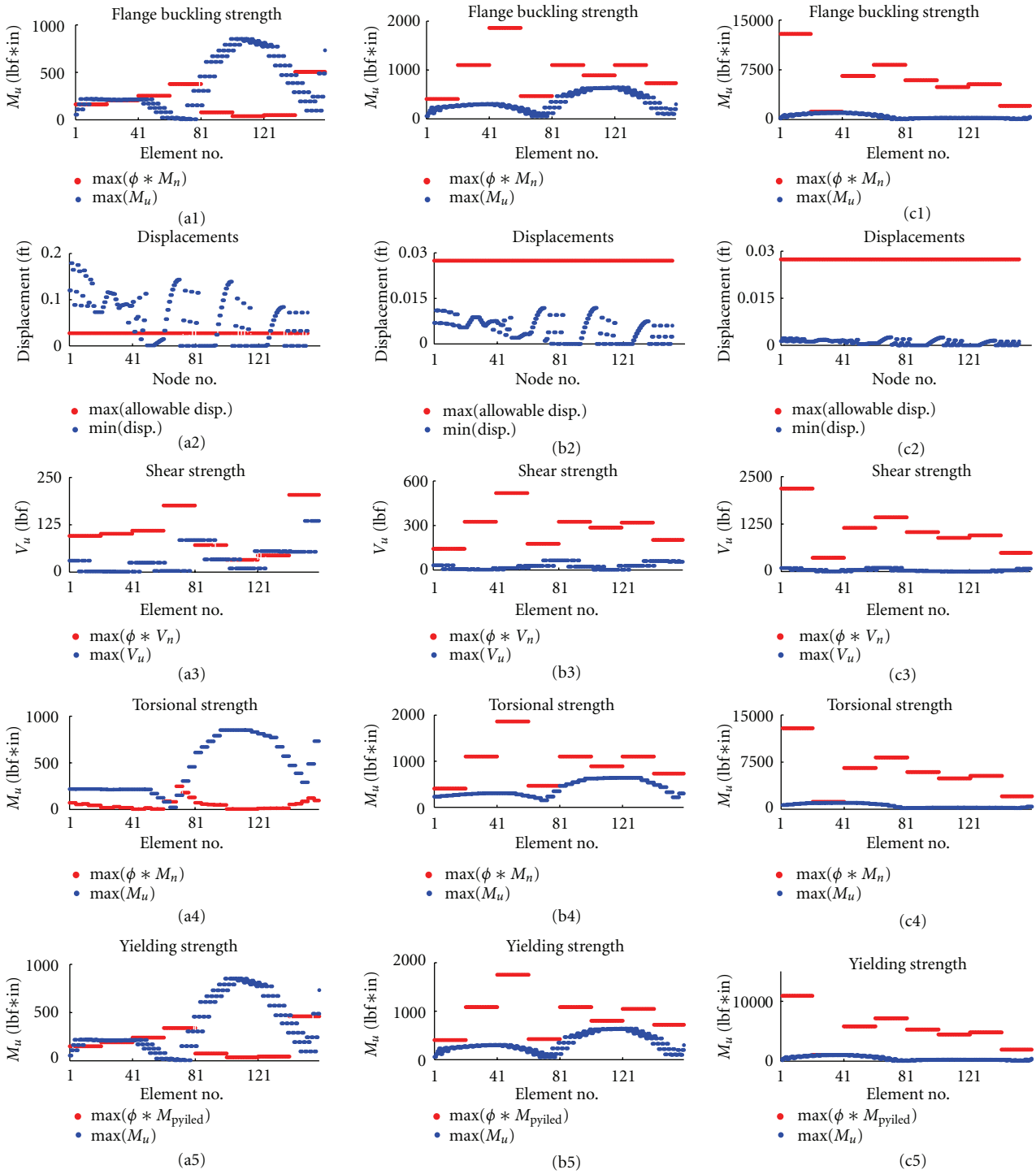

Figure 10: Strengths and displacements of random penalized solutions corresponding to minimum displacement (a1)–(a5), unpenalized solutions corresponding to maximum displacement (b1)–(b5), and maximum weight (c1)–(c5) (see Figure 9).

of the bigger cross-sectional properties for design variables. Furthermore, a common point of these strengths obtained by both panelized and unpenalized solutions corresponding to the maximum displacement is that the yielding limit state has a big impact on the flange buckling, torsional and yielding strengths (see Figures 6(a1), 6(a4), and 6(a5) and 6(b1), 6(b4), and 6(b5)).

6.2. Design Example 2: A Grid System with Five Bays. A grillage system with 160 grid members and 152 nodes is shown in Figure 7. This grillage system is almost 10-times larger than first design example. Grid members are linked in 8 separate groups, resulting in total four design variables in x direction and total four design variables in y direction. According to this linkage system, members (1–

Table 4: Values of measurement quantities obtained by "Eval. Number = 1,000" and "Pop. Size = 50" for design example 2.

C. no.	IGD				HV				Spread			
	AbYSS	NSGAII	PESAII	SPEAII	AbYSS	NSGAII	PESAII	SPEAII	AbYSS	NSGAII	PESAII	SPEAII
	Means											
1	0.2691	0.6444	0.6619	0.2648	0.7136	0.3225	0.8378	0.5906	0.9937	0.9823	0.9574	0.9883
2	0.1887	0.6476	0.3502	0.3181	0.6183	0.5523	0.7391	0.6604	0.9329	*0.9789*	0.9246	0.9962
3	0.2875	0.6790	0.6620	0.1192	0.3433	0.5493	0.3569	0.3488	0.9727	0.9884	0.9861	0.9713
4	0.0911	0.6358	0.4162	0.6456	0.1248	0.3304	0.6627	0.4513	0.9493	0.9995	0.9891	0.9223
5	*0.0156*	0.7093	0.2564	0.4795	**0.9158**	0.3606	0.2815	0.2409	*0.9206*	0.9954	0.9394	0.9345
6	0.6834	*0.2583*	0.6135	0.6393	0.6465	*0.6158*	0.2304	0.7150	0.9296	0.9879	0.9397	0.9976
7	0.5466	0.4501	**0.0118**	0.5447	0.8332	0.4923	0.7111	*0.8767*	0.9889	0.9828	*0.9295*	0.9274
8	0.4257	0.4587	0.5407	*0.0239*	0.3983	0.3278	*0.8968*	0.2815	0.9900	0.9970	0.9456	**0.9154**
	Standard deviations corresponding to best means and assessment of significance levels according to statistical tests											
	0.0113	0.0087	0.0081	0.0105	0.0101	0.0086	0.0078	0.0118	0.0146	0.0127	0.0134	0.0132
			(−)				(−)				(+)	

Table 5: Values of measurement quantities obtained by "Eval. Number = 5,000" and "Pop. Size = 100" for design example 2.

C. no.	IGD				HV				Spread			
	AbYSS	NSGAII	PESAII	SPEAII	AbYSS	NSGAII	PESAII	SPEAII	AbYSS	NSGAII	PESAII	SPEAII
	Means											
1	*0.0078*	0.0205	0.0196	0.0144	0.8935	0.4759	0.6101	0.3714	**0.8356**	*0.9425*	0.9759	0.9108
2	0.0154	0.0216	0.0073	0.0206	0.4658	*0.9278*	0.2036	0.4564	0.9852	0.9998	0.8627	0.8852
3	0.0155	0.0182	0.0098	0.0198	**0.9419**	0.6556	*0.9395*	*0.9400*	0.8749	0.9976	0.9044	*0.8672*
4	0.0196	0.0193	**0.0071**	0.0161	0.4945	0.6204	0.8622	0.7424	0.8564	0.9875	*0.8359*	0.9132
5	0.0170	0.0216	0.0167	*0.0072*	0.8976	0.2828	0.4429	0.9374	0.8998	0.9508	0.8497	0.9224
6	0.0133	*0.0100*	0.0093	0.0102	0.2886	0.2052	0.5480	0.5134	0.8705	0.9820	0.9869	0.8844
7	0.0103	0.0117	0.0086	0.0089	0.2690	0.4391	0.5669	0.2409	0.8648	0.9926	0.9053	0.9773
8	0.0088	0.0156	0.0172	0.0149	0.5942	0.8762	0.6804	0.2600	0.8942	0.9521	0.9316	0.8775
	Standard deviations corresponding to best means and assessment of significance levels according to statistical tests											
	0.0048	0.0064	0.0027	0.0062	0.0038	0.0075	0.0074	0.0062	0.0880	0.0101	0.0980	0.0992
			(+)				(−)				(+)	

Table 6: Values of measurement quantities obtained by "Eval. Number = 1,000" and "Pop. Size = 50" for design example 3.

C. no.	IGD				HV				Spread			
	AbYSS	NSGAII	PESAII	SPEAII	AbYSS	NSGAII	PESAII	SPEAII	AbYSS	NSGAII	PESAII	SPEAII
	Means											
1	0.7590	0.6401	0.3972	0.3320	0.7128	0.2029	0.1523	0.1647	0.9763	0.9998	0.9883	0.9851
2	0.9933	0.6522	0.4794	0.7487	0.8256	*0.5898*	0.3523	0.2716	0.9929	0.9984	0.9962	0.9903
3	0.3567	0.8270	0.5650	0.6444	**0.9485**	0.3551	*0.9373*	0.3144	0.9904	0.9999	*0.9856*	0.9965
4	0.7529	0.8842	0.4896	0.1692	0.6894	0.5478	0.9319	0.6061	**0.9678**	0.9984	0.9941	*0.9705*
5	**0.0258**	0.7006	0.2698	0.9522	0.5309	0.2025	0.7388	0.6775	0.9764	0.9986	0.9880	0.9710
6	0.5970	*0.4879*	0.9897	0.5433	0.1889	0.5132	0.7572	0.7575	0.9869	0.9979	0.9997	0.9827
7	0.4306	0.9367	0.1837	*0.0358*	0.4930	0.5698	0.4635	*0.9287*	0.9685	*0.9978*	0.9938	0.9714
8	0.7307	0.8602	*0.0204*	0.5786	0.5595	0.3736	0.8420	0.4111	0.9761	0.9986	0.9960	0.9804
	Standard deviations corresponding to best means and assessment of significance levels according to statistical tests											
	0.0205	0.0258	0.0227	0.0187	0.0403	0.0327	0.0512	0.0209	0.0208	0.0158	0.0257	0.0128
			(−)				(−)				(−)	

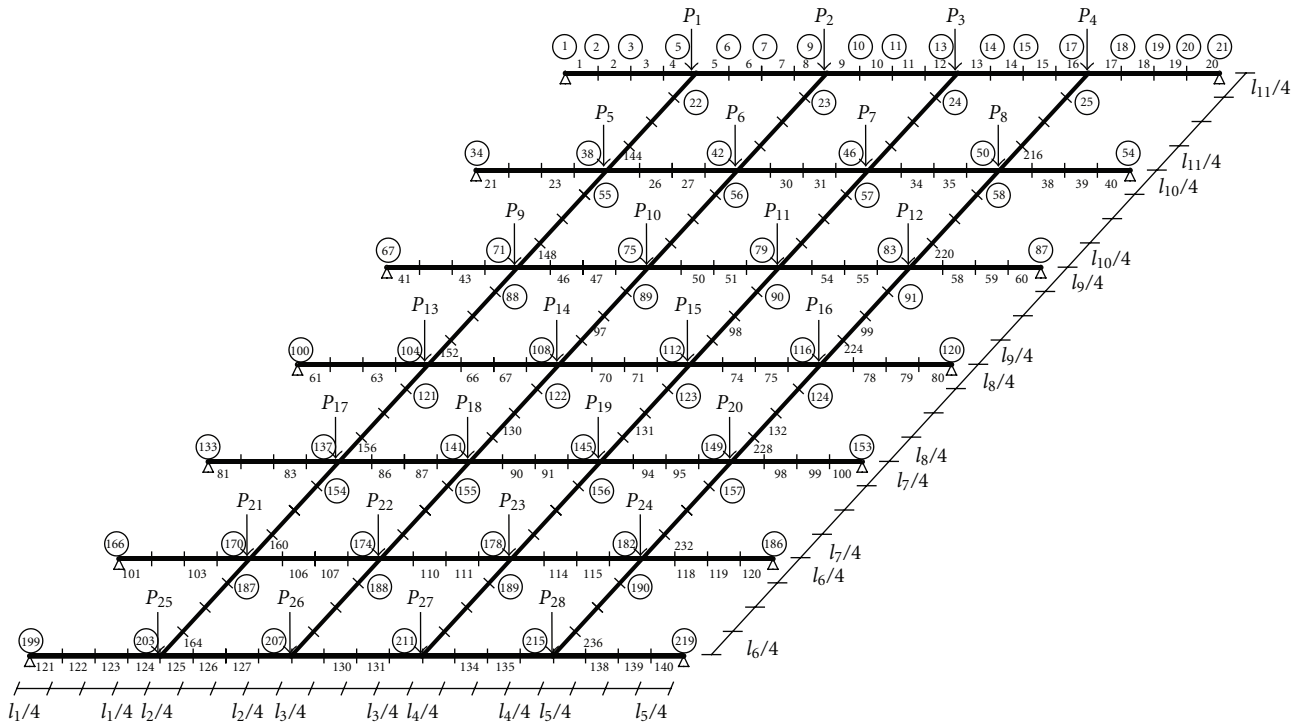

Figure 11: Geometry of 236-member grid structure including locations of point loads.

Table 7: Values of measurement quantities obtained by "Eval. Number = 5,000" and "Pop. Size = 100" for design example 3.

C. no.	IGD				HV				Spread			
	AbYSS	NSGAII	PESAII	SPEAII	AbYSS	NSGAII	PESAII	SPEAII	AbYSS	NSGAII	PESAII	SPEAII
	Means											
1	**0.0101**	0.0225	0.0198	0.0157	**0.9657**	0.9199	0.8154	0.8459	**0.8168**	*0.9494*	*0.8772*	*0.8885*
2	0.0180	*0.0180*	0.0195	0.0213	0.9229	0.9360	0.9430	0.9070	0.9554	0.9498	0.9281	0.9461
3	0.0158	0.0184	0.0233	*0.0140*	0.9174	0.8776	*0.9623*	0.9582	0.8481	0.9586	0.8806	0.9272
4	0.0180	0.0198	*0.0124*	0.0148	0.9292	0.9475	0.8601	*0.9626*	0.9224	0.9556	0.8939	0.9258
5	0.0154	0.0223	0.0212	0.0174	0.8212	0.9346	0.9198	0.8180	0.9369	0.9527	0.9491	0.9320
6	0.0149	0.0192	0.0164	0.0148	0.8577	*0.9592*	0.8790	0.9425	0.9531	0.9583	0.8998	0.9146
7	0.0204	0.0207	0.0153	0.0143	0.8389	0.9020	0.8794	0.8513	0.8995	0.9581	0.9249	0.9582
8	0.0102	0.0193	0.0192	0.0215	0.8378	0.8793	0.8332	0.8653	0.9040	0.9499	0.9373	0.8886
	Standard deviations corresponding to best means and assessment of significance levels according to statistical tests											
	0.0079	0.0084	0.0128	0.0162	0.0138	0.0174	0.0181	0.0219	0.0142	0.0209	0.0251	0.0326
			(+)				(−)				(+)	

20), (21–40), (41–60), (61–80), (81–100), (101–120), (121–140), and (141–160) are linked to represent design variables $1, 2, 3, \ldots, 8$ respectively. Magnitude of loads P_1–P_{16} is equal to 49.46 kipf (219.998 kN). Lengths of spans are $l_1 = l_2 = l_4 = l_5 = 7.220$ ft (2.200 m), $l_3 = 8.220$ ft (2.505 m), $l_6 = l_7 = l_8 = l_9 = l_{10} = 7.870$ ft (2.398 m). The value of allowable displacement is constrained as (8.22/300 = 0.0274 ft; 8.3515 mm).

The pareto fronts of a set of random Nondominated solutions obtained by both use of an increased population size and evolution number and AbYSS, NSGAII, PESAII, and SPEAII are depicted in Figures 8(a) and 8(b1)–8(b4). The means of quality indicator values, standard deviations values corresponding to best means and assessment of significance levels according to statistical tests are reported in Tables 4 and 5. Examining the values of quality indicators tabulated in Tables 4 and 5, it is seen that the lower evolution number and population size decrease the quality degree of optimal designations leading to obtain an inconsistent statistical confidence among quality indicators. However, the quality degree of optimal designations is elevated associated by an increase in the evolution number and population size. According to the quality indicator values, AbYSS (Case 1) succeeded to obtain a lower spread 0.8356 and a higher

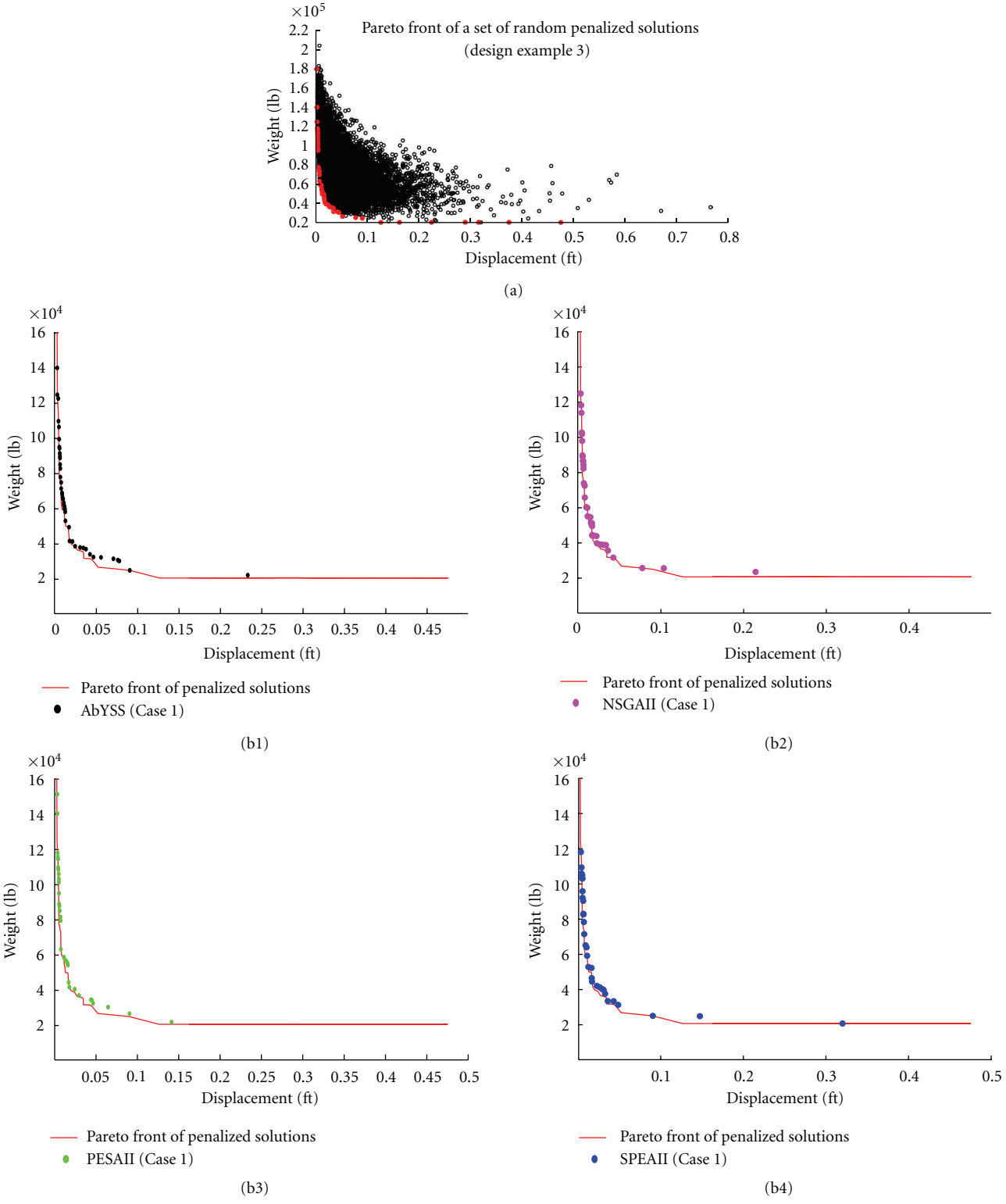

FIGURE 12: Pareto fronts of a set of random nondominated solutions obtained by use of an increased population size and evolution number (a) and AbYSS, NSGAII, PESAII, and SPEAII (b1)–(b4).

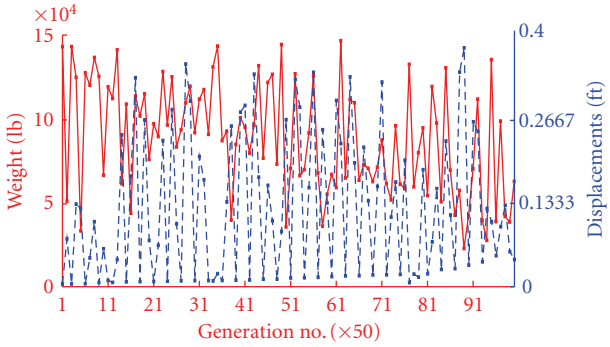

Figure 13: Convergence history obtained by AbYSS (Case 1).

hyper-volume value 0.9419 compared to NSGAII, PESAII, and SPEAII. It is also observed that a higher optimality degree is obtained by use of either lower parameter values of evolutionary operators in conjunction with a decreased evolution number and population size or higher ones in conjunction with an increased evolution number a population size. This claim is approved by examining the quality indicator values with bold and italic characters obtained by Cases 1–4, which indicate a usage of lower evolution number and population size and Cases 5–8, which indicate a usage of higher evolution number and population size (see Tables 4 and 5). Considering the best spread values, the pareto fronts obtained by four MOAs employed are compared with both each other and the pareto front obtained by use of higher population size and evolution number (Figure 8(b1)–8(b4)). The convergence history of the optimizer AbYSS (Case 1) with the best spread value 0.8067 is presented in Figure 9 with two axes. A designation with (weight = 13584.2465 lb (6161.7105 kg) and displacement = 0.0798 ft (24.3230 mm)) is obtained in a generation of no. = 4257 located in a segment of no. 85 with an interval ($80 \times 50 = 4000$ and $90 \times 50 = 4500$).

The strength values of grid members are displayed considering penalized designation corresponding to a maximum displacement (weight = 9888.9999 lb (4485.5749 kg) and displacement = 0.1633 ft (49.7738 mm); see Figure 10 (a1)–10(a5)) and unpenalized designations corresponding to a maximum displacement (weight = 32718.4000 lb (14840.8165 kg) and displacement = 0.0125 ft (3.81 mm)) and a maximum weight (weight = 102588.7500 lb (46533.4742 kg) and displacement = 0.0025 ft (0.762 mm); see Figures 10(b1)–10(b5) and 10(c1)–10(c5)). Whereas the penalized designation corresponding to the maximum displacement contains a W-section set (W14×38, W12×45, W12×53, W18×55, W12×22, W6×8.5, W6×20, and W18×71), the unpenalized designations corresponding to the maximum displacement and weight are represented by W-section sets (W12×87, W24×131, W33×152, W10×112, W24×131, W12×170, W21×132, W14×132) and (W40×149, W12×210, W36×441, W36×529, W36×395, W36×330, W36×361, and W27×194), respectively. An increase in the displacement values causes convergence in the flange bucking, torsional, and yielding-related strength values to their related yielding limit values. Hence, the distribution of these strengths on the grid members becomes more close to their limit state values (see Figure 10(a1), 10(a4) and 10(a5) and 10(b1), 10(b4), and 10(b5)). An increase in the weight of grid structure leads to an elevation in the limit state values (see Figure 10(c1)–10(c5)).

6.3. Design Example 3: A Grid System with Five and Six Bays. This grillage system with 236 members and 219 joint points has the highest complexity among design examples due to both lower number of support points constructed to carry a large grillage area and higher number of members and joints (see Figure 11). Grid members (1–20), (21–40), (41–60), (61–80), (81–100), (101–120), and (121–140) are linked to represent design variables $1, 2, \ldots, 7$ in x direction while design variables 8, 9, 10, and 11 in y direction are assigned to lattice beams which are denoted by $(141, 145, 149, \ldots, 221, 225, 229,$ and $233)$, $(142, 146, 150, \ldots, 222, 226, 230,$ and $234)$, $(143, 147, 151, \ldots, 223, 227, 231,$ and $235)$, and $(144, 148, 152, \ldots, 224, 228, 232,$ and $236)$. Magnitude of loads (P_1–P_4 and P_{25}–P_{28}), (P_5–P_8 and P_{21}–P_{24}), (P_9–P_{12} and P_{17}–P_{20}), and (P_{13}–P_{16}) are taken as 24.730 kipf (109.999 kN), 35.970 kipf (159.995 kN), 38.210 kipf (169.959 kN) and 42.710 kipf (189.974 kN). Lengths of spans are equal to $l_1 = l_5 = 7.550$ ft (2.30 m), $l_2 = l_4 = l_6 = l_{11} = 7.870$ ft (2.399 m), $l_3 = 8.200$ ft (2.499 m), $l_7 = l_{10} = 8.530$ ft (2.599 m), and $l_8 = l_9 = 9.180$ ft (2.798 m). The value of allowable displacement is constrained as (9.18/300 = 0.0306 ft; 9.3268 mm).

The pareto fronts of a set of random Nondominated solutions obtained by both use of an increased population size and evolution number and AbYSS, NSGAII, PESAII, and SPEAII are depicted in Figures 12(a) and 12(b1)–12(b4). The quality indicator related-quantities including statistical test results are reported in Tables 6 and 7. According to tabulated valued in Tables 6 and 7, a decrease in the evolution number and population size causes the quality indicator values to be poor and hence statistical confidence to be inconsistent. Considering the indicator values in Table 7, it is obvious that AbYSS (Case 1) shows a better computational performance by obtaining a lower spread 0.8168 and a higher hyper-volume value 0.9657 compared to NSGAII, PESAII, and SPEAII. Also, the quality indicators obtained by PESAII and SPEAII are better than NSGAII. According to the convergence history of AbYSS (Case 1) with the best spread value 0.8168 presented in Figure 13, a designation with (weight = 22354.1046 lb (10139.6512 kg) and displacement = 0.2331 ft (71.0488 mm)) is obtained in a generation of no. = 4461 located in a segment of no. 89 with a interval ($80 \times 50 = 4000$ and $90 \times 50 = 4500$).

The strength values of grid members are displayed considering penalized designation corresponding to a maximum displacement (weight = 36375.3700 lb (16499.5902 kg) and displacement = 0.7651 ft (233.2024 mm); see Figure 14 (a1)–14(a5)) and unpenalized designations corresponding to a maximum displacement (weight = 44028.4600 lb (19970.9735 kg) and displacement = 0.02142 ft (6.528 mm))

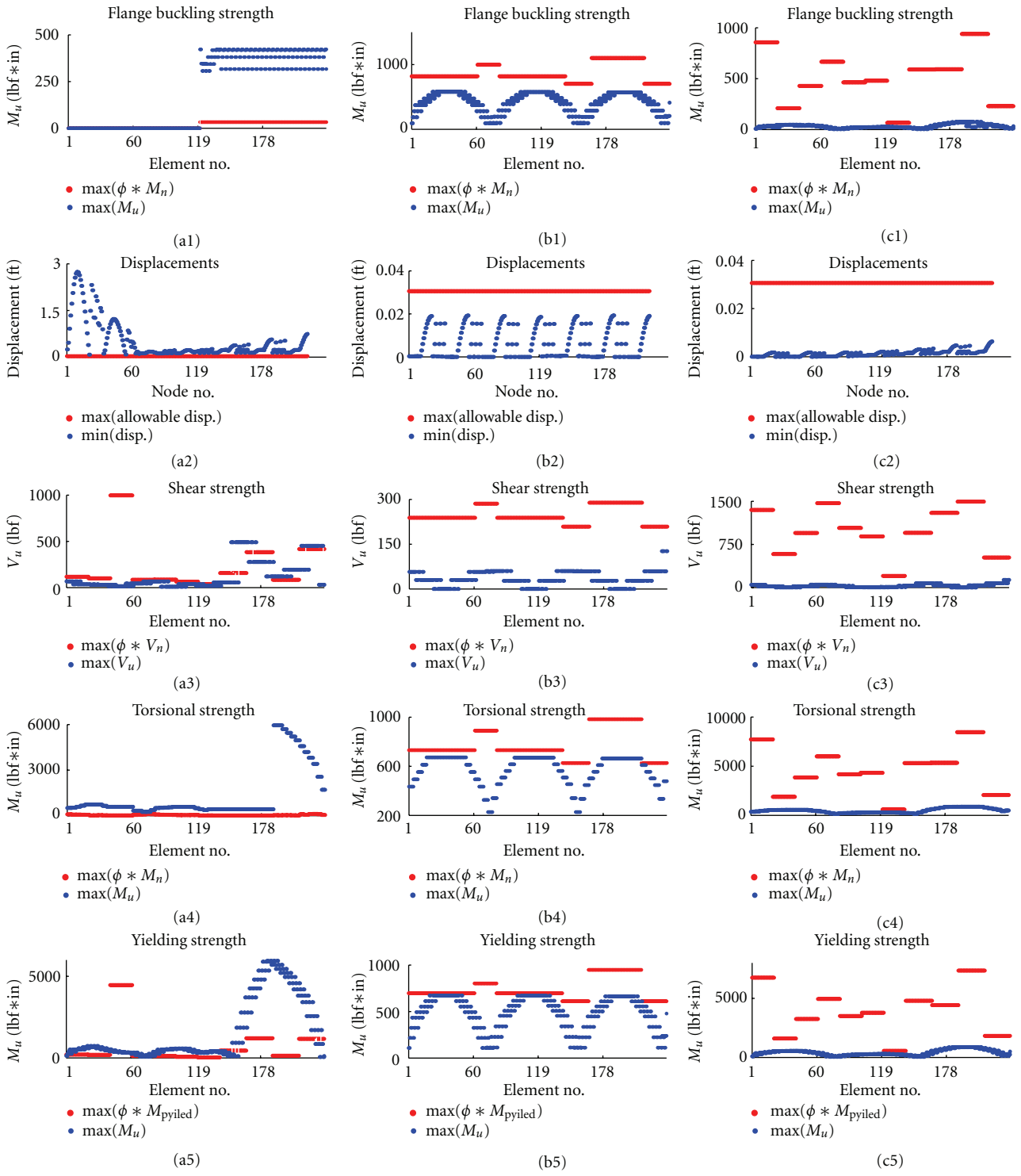

FIGURE 14: Strengths and displacements of random penalized solutions corresponding to minimum displacement (a1)–(a5), unpenalized solutions corresponding to maximum displacement (b1)–(b5), and maximum weight (c1)–(c5) (see Figure 13).

and a maximum weight (weight = 176334.6800 lb (79984.0654 kg) and displacement = 0.0066 ft (2.0116 mm); see Figures 14(b1)–14(b5) and 14(c1)–14(c5)). Whereas the penalized designation corresponding to the maximum displacement contains a W-section set (W16×40, W12×45, W30×391, W14×30, W12×30, W12×19, W8×15, W12×96, W18×175, W10×39, and W30×116), the unpenalized designations corresponding to the maximum displacement and weight are represented by W-section sets (W18×106, W18×106, W18×106, W12×170, W18×106, W18×106,

W18×106, W18×97, W21×122, W21×122, and W18×97), and (W40×503, W12×305, W14×500, W14×730, W14×550, W40×278, W16×100, W36×361, W14×665, W40×593, and W14×311), respectively. Examining Figure 14(a1)–14(a5), it is seen that torsional and yielding strengths play a bigger and more important role in the bearing capacity of grid structure compared to the other strengths. A similar result as in the application of design examples 1 and 2 is obtained in this application example: a decrease in the displacement values causes the flange bucking, torsional, and yielding-related strengths to obtain highly near to their related yielding limit state values. Using the steel profiles with larger cross-sectional properties leads to an increase in both weight of grid structure and limit state values.

7. Conclusion

In this study, the designs of grillage systems are optimized using the optimization tools named NSGAII, SPEAII, PESAII, and AbYSSS according to the design provisions of LRFD-AISC Ver.13 specification. Hence, the computational performances of the MOAs employed are not only evaluated but the change in the strength of gird members in conjunction with joint displacements is also displayed. In order to assess the computational performance of MOAs, the various quality indicators, IGD, HV, and spread are computed considering the application of three design examples with an order of increasing complexity degree and evaluated their statistical confidences according to outcomes of statistical tests. According to the evaluation of quality indicators and optimal designations, the following results are observed.

(i) According to the values of quality indicators, AbYSS shows better computational performance compared to SPEAII, PESAII, and NSGAII. Moreover, NSGAII obtains the worst values of quality indicators than SPEAII and PESAII, whose computational performances are almost equal.

(ii) An efficient exploration of search space is only provided by usage of an increased evolution number and population size. Otherwise, the outcomes from statistical tests point out an inconsistent relation between quality indicators obtained by use of a decreased evolution number and population size.

(iii) An increase in the parameter values of evolutionary operators in conjunction with the evolution number and population size leads to an improvement in the convergence degree of optimal designations.

(iv) In conjunction with increasing the evolution number and populations size, the degrees of quality indicators are improved by use of (higher *crossover probability and crossover distribution index*—higher *mutation probability and mutation distribution index*—higher *reference sets and archive size*) for the evolutionary operators of AbYSS, and (lower *crossover probability and crossover distribution index*—lower *mutation probability and mutation distribution index*—higher *archive size*) or (higher *crossover probability and crossover distribution index*—lower *mutation probability and mutation distribution index*—higher *archive size*) for the evolutionary operators of SPEAII and PESAII.

(v) A decrease in the joint displacement correspondingly causes the values of flange buckling, torsional, and yielding strengths to obtain near to their related limit state values. In this regard, the bearing capacity of grid structure has to be kept in the upper levels against any drastic decrease in joint displacements. Therefore, using a multi-objective optimization algorithm becomes a reasonable approach for the optimal design of grillage systems.

In the next work, the effect of using the different evolutionary parameter values on the quality degree of optimal designations will be evaluated. Furthermore, the proposed MOAs will be hybridized with both each other and the other evolutionary optimization algorithms in order to both reduce the evolutionary computational cost spent to obtain Nondominated solutions and improve the curves of pareto fronts.

Nomenclature for AISC_LRFD Ver.13 Specification

b_f: Flange width
C_b: Lateral-torsional buckling modification factor for non-uniform moment diagrams
E: Elasticity modules
F_{cr}: Critical stress
F_y: Specified minimum yield stress
h: Clear distance between flanges
h_0: Distance between flange centroids
I_y: Out-of-plane moment of Inertia
J_c: Torsional constant
k_c: Coefficient for slender unstiffened elements
k_v: Web-plate buckling coefficient
L_p: Limiting laterally unbraced length for the limit state of yielding
L_b: Distance between braces
L_r: Limiting laterally unbraced length for the limit state of inelastic lateral-torsional buckling
M_n: Nominal flexural strength
M_p: Plastic bending moment
M_A: Absolute value of monet at quarter point of unbraced segment
M_B: Absolute value of monet at centerline point of unbraced segment
M_C: Absolute value of monet at three-quarter point of unbraced segment
r_y: Radius of gyration about y-axes
r_{ts}: Effective radius of gyration used in the determination of L_r for lateral-torsional buckling limit state
S_x: Elastic section modules about principal axes
t_f: Thickness of flange

t_w: Web thickness
Z_x: Plastic section modules about principal axes
λ_p: Limiting slenderness parameter for compact element
λ_{pf}: Limiting slenderness parameter for compact flange
λ_{rf}: Limiting slenderness parameter for compact web
λ: Slenderness parameter.

Acknowledgments

The author would like to thank Professor Dr. Antonio J. Nebro, Prof. Dr. Juan J. Durillo, and their team members for releasing the source code of JMETAL to execute computational procedures of multi-objective optimization methods. He thanks reviewers for their valuable comments and recommendations about revision of this paper. He also thanks Kadirli Municipality of Osmaniye for their support to this paper.

References

[1] J. D. Schaffer, *Multiple objective optimization with vector evaluated genetic algorithms*, Ph.D. thesis, Vanderbilt University, 1984.

[2] I. Das and J. E. Dennis, "A closer look at drawbacks of minimizing weighted sums of objectives for pareto set generation in multicriteria optimization problems," *Structural Optimization*, vol. 14, no. 1, pp. 63–69, 1997.

[3] A. Hertz, B. Jaumard, C. Ribeiro, and W. F. Filho, "A multicriteria tabu search approach to cell formation problems in group technology with multiple objectives," *RAIRO—Operations Research*, vol. 28, no. 3, pp. 303–328, 1994.

[4] D. E. Goldberg, *Genetic Algorithms in Search. Optimization and Machine Learning*, Addison-Wesley Publishing, Massachusetts, Mass, USA, 1989.

[5] N. Srinivas and K. Deb, "Multiobjective optimization using nondominated sorting in genetic algorithms," *Evolutionary Computation*, vol. 2, no. 3, pp. 221–248, 1994.

[6] J. N. Horn, A. L. Nafpliotis, and D. E. Goldberg, "A niched Pareto genetic algorithm for multiobjective optimization," in *Proceedings of the First IEEE Conference on Evolutionary Computation, IEEE World Congress on Computational Intelligence*, pp. 82–87, IEEE Service Center, Piscataway, NJ, USA, Jun 1994.

[7] C. M. Fonseca and F. J. Fleming, "Genetic algorithms for multiobjective optimization: formulation, discussion and generalization," in *Proceedings of the Fifth International Conference on Genetic Algorithms*, S. Forrest, Ed., pp. 416–423, Morgan Kauffman, San Mateo, Calif, USA, June 1993.

[8] M. Tanaka and T. Tanino, "Global optimization by the genetic algorithm in a multiobjective decision support system," in *Proceedings of the 10th International Conference on Multiple Criteria Decision Making*, pp. 261–270, Taipei, China, July 1992.

[9] K. Deb, *Multi-Objective Optimization Using Evolutionary Algorithms*, John Wiley & Sons, Chichester, UK, 2001.

[10] E. Zitzler and L. Thiele, "Multiobjective evolutionary algorithms: a comparative case study and the strength Pareto approach," *IEEE Transactions on Evolutionary Computation*, vol. 3, no. 4, pp. 257–271, 1999.

[11] J. D. Knowles and D. W. Corne, "Approximating the nondominated front using the Pareto archived evolution strategy," *Evolutionary Computation*, vol. 8, no. 2, pp. 149–172, 2000.

[12] K. Deb and T. Goel, "Controlled elitist non-dominated sorting genetic algorithms for better convergence," *Lecture Notes in Computer Science*, vol. 1993, pp. 67–81, 2001.

[13] S. S. Rao, V. B. Venkayya, and N. S. Khot, "Optimization of actively controlled structures using goal programming techniques," *International Journal for Numerical Methods in Engineering*, vol. 26, no. 1, pp. 183–197, 1988.

[14] J. P. Ignizio, *Goal Programming and Extensions*, Heath, Boston, Mass, USA, 1976.

[15] S. S. Rao and T. I. Freiheit, "Modified game theory approach to multiobjective optimization," *Journal of Mechanisms, Transmissions, and Automation in Design*, vol. 113, no. 3, pp. 286–291, 1991.

[16] M. Sunar and R. Kahraman, "A comparative study of multiobjective optimization methods in structural design," *Turkish Journal of Engineering and Environmental Sciences*, vol. 25, no. 2, pp. 69–78, 2001.

[17] J. Koski, "Defectiveness of weighting method in multicriterion optimization of structures," *Communications in Numerical Methods in Engineering*, vol. 1, no. 6, pp. 333–337, 1985.

[18] I. Das and J. E. Dennis, "A closer look at drawbacks of minimizing weighted sums of objectives for Pareto set generation in multicriteria optimization problems," *Structural Optimization*, vol. 14, no. 1, pp. 63–69, 1997.

[19] A. Messac and C. A. Mattson, "Generating well-distributed sets of Pareto points for engineering design using physical programming," *Optimization and Engineering*, vol. 3, no. 4, pp. 431–450, 2002.

[20] I. Y. Kim and O. L. Weck, "Adaptive weighted-sum method for bi-objective optimization: Pareto front generation," *Structural and Multidisciplinary Optimization*, vol. 29, no. 2, pp. 149–158, 2005.

[21] A. Molina-Cristobal, L. A. Griffin, P. J. Fleming, and D. H. Owens, "Multiobjective controller design: optimising controller structure with genetic algorithms," in *Proceedings of the 16th IFAC World Congress on Automatic Control*, Prague, Czech Republic, July 2005.

[22] C. A. C. Coello and N. C. Cortes, "Solving multiobjective optimization problems using an artificial immune system," *Genetic Programming and Evolvable Machines*, vol. 6, no. 2, pp. 163–190, 2005.

[23] M. Guntsch, *Ant algorithms in stochastic and multi-criteria environments*, Ph.D. thesis, Department of Economics and Business Engineering, University of Karlsruhe, Germany, 2004.

[24] C. A. Coello and P. G. Toscano, "Multiobjective optimization using a micro-genetic algorithm," in *Proceedings of the Genetic And Evolutionary Computation Conference, (GECCO '01)*, L. Spector et al., Ed., pp. 174–282, Morgan Kaufmann, San Francisco, Calif, USA, August 2001.

[25] R. M. Janga and K. D. Nagesh, "An efficient multi-objective optimization algorithm based on swarm intelligence for engineering design," *Engineering Optimization*, vol. 39, no. 1, pp. 49–68, 2007.

[26] N. Keerativuttitumrong, N. Chaiyaratana, and V. Varavithya, "Multi-objective co-operative co-evolutionary genetic algorithm," *Lecture Notes in Computer Science*, vol. 2439, pp. 288–297, 2002.

[27] C. M. Fonseca and P. J. Fleming, "Genetic algorithms for multiobjective optimization: formulation, discussion and generalization," in *Proceedings of the 5th International Conference*

on Genetic Algorithms, pp. 416–423, Urbana-Champaign, Ill, USA, June 1993.

[28] J. Horn and N. Nafpliotis, "Multiobjective optimization using the niched Pareto genetic algorithm," IlliGAL Report 93005, Illinois Genetic Algorithms Laboratory, University of Illinois, Urbana-Champaign, Ill, USA, 1993.

[29] A. R. Khorsand and M. R. Akbarzadeh, "Multi-objective meta level soft computing-based evolutionary structural design," *Journal of the Franklin Institute*, vol. 344, no. 5, pp. 595–612, 2007.

[30] M. P. Saka, A. Daloglu, and F. Malhas, "Optimum spacing design of grillage systems using a genetic algorithm," *Advances in Engineering Software*, vol. 31, no. 11, pp. 863–873, 2000.

[31] F. Erdal and M. P. Saka, "Effect of beam spacing in the harmony search based optimum design of grillages," *Asian Journal of Civil Engineering*, vol. 9, no. 3, pp. 215–228, 2008.

[32] M. P. Saka and F. Erdal, "Harmony search based algorithm for the optimum design of grillage systems to LRFD-AISC," *Structural and Multidisciplinary Optimization*, vol. 38, no. 1, pp. 25–41, 2009.

[33] J. K. Nelson and J. C. McCormac, *Structural Analysis 3E WSE: Using Classical and Matrix Methods*, John Wiley & Sons, New York, NY, USA, 2003.

[34] http://jmetal.sourceforge.net/.

[35] K. Deb, S. Agrawal, A. Pratab, and T. Meyarivan, "A fast elitist non-dominated sorting genetic algorithm for multi-objective optimization:NSGA-II," in *Proceedings of the 6th International Conference on Parallel Problem Solving from Nature, (PPSN '00)*, M. Schoenauer, K. Deb, G. Rudolph et al., Eds., pp. 849–858, Paris, France, September 2000.

[36] K. Deb, A. Pratap, S. Agarwal, and T. Meyarivan, "A fast and elitist multiobjective genetic algorithm: NSGA-II," *IEEE Transactions on Evolutionary Computation*, vol. 6, no. 2, pp. 182–197, 2002.

[37] K. Deb, *Multi-Objective Optimization Using Evolutionary Algorithms*, John Wiley & Sons, New York, NY, USA, 2001.

[38] D. W. Corne, J. D. Knowles, and M. J. Oates, "The Pareto envelope-based selection algorithm for multiobjective optimization," in *Proceedings of the 6th International Conference on Parallel Problem Solving from Nature, (PPSN '00)*, M. Schoenauer, K. Deb, G. Rudolph et al., Eds., pp. 839–848, Paris, France, September 2000.

[39] D. W. Corne, N. R. Jerram, J. D. Knowles, and M. J. Oates, "PESA-II: regionbased selection in evolutionary multiobjective optimization," in *Proceedings of the the Genetic and Evolutionary Computation Conference, (GECCO '01)*, L. Spector, E. D. Goodman, A. Wu et al., Eds., pp. 283–290, San Francisco, Calif, USA, July 2001.

[40] K. Deb, M. Mohan, and S. Mishra, "Towards a quick computation of well-spread pareto-optimal solutions," in *Proceedings of the Second International Conference on Evolutionary Multi-Criterion Optimization, (EMO '03)*, C. M. Fonseca, P. J. Fleming, E. Zitzler, K. Deb, and L. Thiele, Eds., pp. 222–236, Faro, Portugal, April, 2003.

[41] A. J. Nebro, F. Luna, E. Alba, B. Dorronsoro, J. J. Durillo, and A. Beham, "AbYSS: adapting scatter search to multiobjective optimization," *IEEE Transactions on Evolutionary Computation*, vol. 12, no. 4, pp. 439–457, 2008.

[42] The MathWorks, "Statistical toolbox User's Guide," 2008.